Deliverable 7.3.6

Multi-scale MR assessment Proof of Concept

Work Package 3

Task 7.3.3

Leader: University of Florence

Project Acronym: RETURN

Project Title: multi-Risk sciEnce for resilienT commUnities undeR a changiNg climate

Project duration: 01/12/2022 – 30/11/2025

Project code: PE00000005 CUP: H93C22000610002

Florence, 31 July 2025

Project coordinator

Domenico Calcaterra (Department of Earth Science, Environment and Resources - University of Naples Federico II)

Spoke coordinator

Fabio Castelli (Civil and Environmental Engineering Department - University of Florence)

Work Package coordinator

Chiara Arrighi (Civil and Environmental Engineering Department - University of Florence)

Task coordinator

Emanuele Intrieri (Earth Science Department - University of Florence)

Working group

Earth Science Department - University of Florence

Silvia Bianchini

Irene Centauro

Alessio Gatto

Emanuele Intrieri

Samuele Segoni

Civil and Environmental Engineering Department - University of Florence

Chiara Arrighi

Fabio Castelli

Architecture Department - University of Florence

Vieri Cardinali

Mario De Stefano

Antonino Maria Marra

Gianfranco Stipo

Marco Tanganelli

CIMA Foundation

Silvia Degli Esposti

Paolo Fiorucci

Giorgio Meschi

Nicolò Perello

Andrea Trucchia

Civil and Environmental Engineering and Architecture Department - University of Cagliari

Marco Cigagna

Donatella Rita Fiorino

Battista Grosso

Elisa Pilia

Francesco Pinna

Giuseppina Vacca

Enrica Vecchi

Table of contents

Summary

1 Introduction

This document is meant as an additional document to the 7.3.6 deliverable "Multi-scale MR assessment Proof of Concept", which consists in the creation of proof of concept multi-risk maps for cultural heritage (CH) at different scales and is the result of the work develop within the framework of task 7.3.3 "Systematic mapping and application of MR analysis for CH, from site to urban to regional and national scales".

Therefore, the following pages provide a short and practical methodology for understanding and replicating the maps at the national scale, regional scale, urban scale and at the scale of a biosphere reserve, considering four types of risk: landslides, floods, earthquakes and wildfires. Earthquake risk and seismic risk are used with the same meaning.

It is worth noting that, since the focus of these guidelines is the CH, consequences on people or the environment are not considered. This means that the risk for a CH building is only referred to the building or asset per se and not to the people that may inhabit it. Risk analyses on people are necessary and must be integrated with assessment on CH, but they are the default kind of risk assessment and are not dealt with in this task.

The analysis begins with the definition of the risk equation, incorporating its fundamental components: hazard, vulnerability, and exposure.

The risk equation is based on the relationship: $R = H \times V \times E$ where:

- R: Risk
- H: Hazard of the event
- V: Vulnerability of the exposed element
- E: Exposure (value) of the element

The hazard represents the probability that an adverse event will occur in a given location with a certain intensity. It is assessed through historical data, geospatial models, and frequency analyses of past events. Vulnerability indicates the degree of damage a cultural heritage asset might sustain in the event of a hazardous occurrence. It depends on structural, material, and typological factors specific to the assets under consideration. Exposure accounts for the spatial distribution of cultural heritage assets and their intrinsic value. This study evaluates exposure based on the cultural significance assigned to each asset.

Risk calculation requires a distinct evaluation of each element in the risk equation. The subsequent sections describe the methodologies and datasets utilized for hazard (H), vulnerability (V), and exposure (E) across all risk types. A uniform methodological approach has been implemented for all four hazards to ensure consistency in the different scale analysis.

2 National scale

While largely used, the term "national" can be misleading. In this case it is used to refers to extension indicatively comprised between 100,000 km^2 and 1,000,000 km^2. Ideally this methodology can be used for cross-border maps, but crossing multiple countries increases the risk of inhomogeneous maps and database which would require further data preparation with respect to the method adopted in this proof of concept. Given its extension, the ubiquitous dissemination of CH assets, and the detailed spatial knowledge about different types of risk, Italy is an optimal proof of concept (PoC) for the proposed methodology.

2.1 Cultural Heritage Database

The database used in this study is provided by the Ministry of Culture (MiC, 2025a) and includes 185,708 georeferenced cultural heritage assets. Each asset is described based on its geographic location, designation (physical description of the asset), typology (e.g., churches, palaces, bell towers, etc.), class (architectural, archaeological, park/garden), and cultural significance. Among the 185,708 assets, only 155,076 (83.5%) have an assigned typology.

The classification based on cultural significance reveals that (Figure 1):

- 76,469 assets (41.18%) are officially recognized as cultural heritage,
- 107,630 (57.96%) have not yet undergone official verification,
- 1,544 (0.83%) are under evaluation,
- 65 (0.04%) have been declared of no cultural interest.

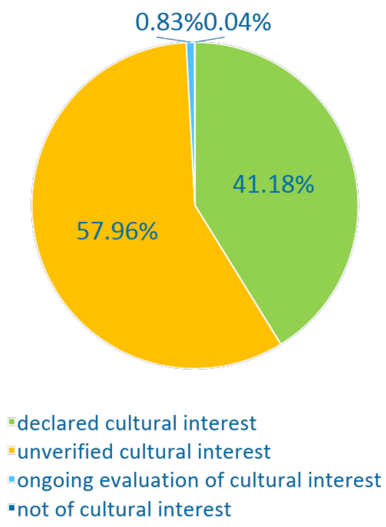

Figure 1. Distribution of the significance of CH within the database.

2.2 Typological Classification

Given that there are 393 different typologies, a matrix was adopted that combines five geometrical classes (tall, equidimensional, small, subterranean, wide) with six function categories of assets (defensive structures, open spaces, infrastructure, etc.), as shown in Table 1, resulting in 30 possible typological combinations. This classification enables a more precise assessment of vulnerability concerning different hazards.

Table 1. The elements at risk have been reclassified from 1A to 6E according to their geometry and category.

		Tall	Equidimensional	Small	Subterranean	Wide
		A	B	C	D	E
Buildings potentially containing valuable items	1	1A	1B	1C	1D	1E
Defensive Structures	2	2A	2B	2C	2D	2E
Civil buildings and artifacts	3	3A	3B	3C	3D	3E
Infrastructure	4	4A	4B	4C	4D	4E
Monuments, remains, and archaeological areas	5	5A	5B	5C	5D	5E
Open spaces, landscapes and associated artifacts, natural monuments	6	6A	6B	6C	6D	6E

2.3 Hazard

2.3.1 Landslide hazard

Concerning landslide hazard, data come from the PAI project by ISPRA (Istituto Superiore per la Protezione e la Ricerca Ambientale) through the IdroGEO portal (ISPRA IdroGEO, 2025). It consists of a shapefile mapping four hazard classes, categorized based on different levels. The four classes are defined based on historical data, satellite data analysis, and in-situ surveys, providing a comprehensive assessment of landslide hazard (Figure 2):

- Low hazard (P1)
- Medium hazard (P2)
- High hazard (P3)
- Very high hazard (P4)

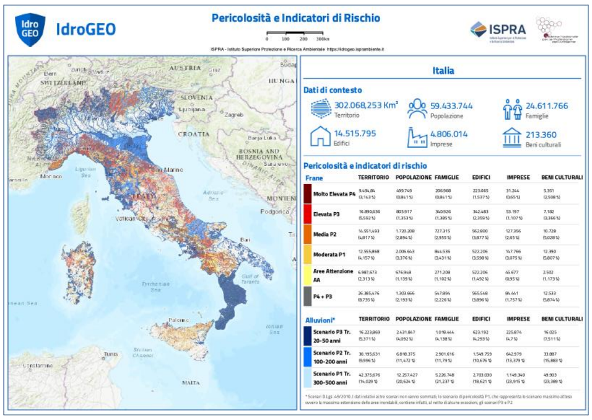

Figure 2. Screenshot from IdroGEO portal (ISPRA IdroGEO, 2025).

A GIS-based "select by location" operation was performed to assign a hazard value to cultural heritage assets. This process identified assets located within the mapped hazard classes. Subsequently, the hazard values were assigned using the "Calculate Field" tool, setting the hazard value based on the selected elements for each class and assigning values ranging from 1 to 4 according to the corresponding hazard level (Figure 3).

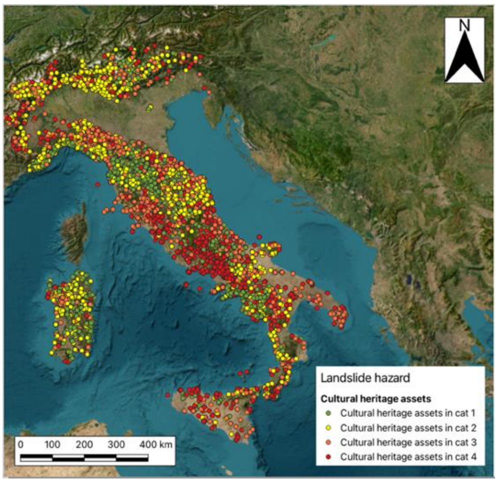

Figure 3. National map showing the landslide hazard for cultural heritage.

2.3.2 Flood hazard

For the flood risk, the maps used derive from the Flood Risk Management Plan (PGRA Piano di Gestione del Rischio di Alluvioni), which categorizes areas into three risk levels based on different probability scenarios:

- High hazard (P3): Areas subject to flooding with a return period of up to 50 years
- Medium hazard (P2): Areas subject to flooding with a return period between 100 and 200 years
- Low hazard (P1): Areas subject to flooding with a return period exceeding 300 – 500 years

This classification is based on the return period of flood events, which indicates the average interval between occurrences of similar magnitude. Similar to the PAI dataset, which identifies areas of landslides hazard, this database was also obtained from ISPRA via the IdroGEO platform (ISPRA IdroGEO, 2025). It includes a detailed shapefile representing three levels of flood hazard. The assignment of hazard values to each cultural asset was carried out through spatial analysis, considering the assets' geographical position in relation to the designated hazard zones. The methodology follows the same approach used for assessing landslide risk. After selecting the assets based on their spatial location within the hazard areas, they were assigned a corresponding hazard value of 1, 2, or 3, depending on the level of flood hazard (Figure 4).

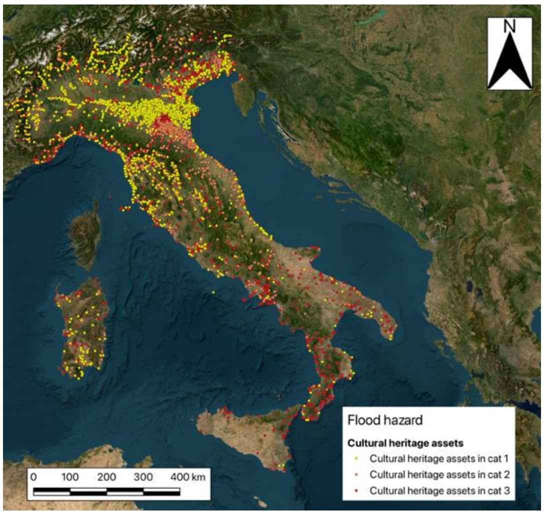

Figure 4. National map showing the flood hazard for cultural heritage.

2.3.3 Earthquake hazard

Concerning the earthquake hazard the initial data pertains to the national mapping of ground acceleration (ag) values provided by the Italian National Institute of Geophysics and Volcanology (INGV, 2025). This open-access dataset encompasses the entire Italian territory and consists of a point shapefile with a grid of points approximately 2.5 km apart, each associated with a corresponding ag value. The employed methodology involved creating a grid with cells measuring 2.5 km on each side, centering each cell on the points from the database, and subsequently rasterizing it. This process resulted in a national-scale map where each cell represents the ag value over an area of 5 km^2. The seismic hazard map at national level provided by INGV has been replotted considering the return period associated with CH buildings. Assuming a nominal life of 50 years and an important class III, a return period of 712 years is obtained for SLV.

The classification of ag values is divided into 12 classes, specified as follows: 0.001-0.025, 0.026-0.050, 0.051-0.075, 0.076-0.100, 0.101-0.125, 0.126-0.150, 0.151-0.175, 0.176-0.200, 0.201-0.225, 0.226-0.250, 0.251-0.275, and 0.276-0.300. To ensure consistency with the hazard classification of other risks, the ag values were grouped into four classes:

- **Class 1:** 0.001-0.075
- **Class 2:** 0.076-0.150
- **Class 3:** 0.151-0.225
- **Class 4:** 0.226-0.300

As for the risks explained above, each CH asset in the database was assigned a corresponding value from 1 to 4 based on its spatial distribution, utilizing the "Point Sampling Tool" command in GIS environment, which extracts raster values at specified point locations. This approach generated a map representing the respective hazard for each point, categorized into four classes, consistent with landslide risk assessment (Figure 5).

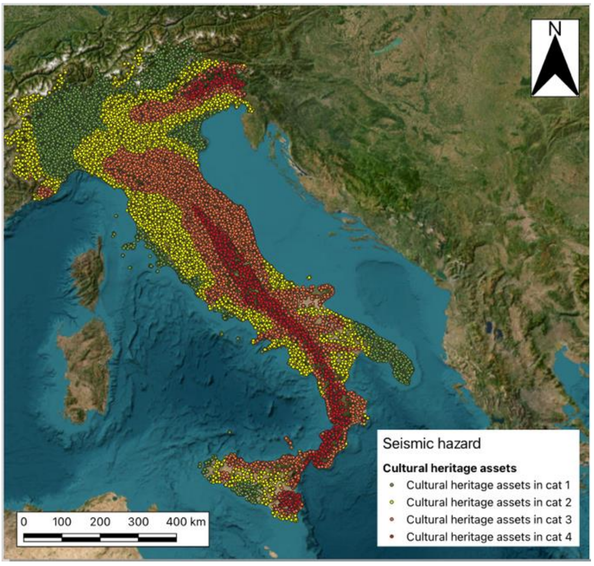

Figure 5. National map showing the seismic hazard for cultural heritage.

2.3.4 Wildfire hazard

Finally, concerning wildfire hazard, it is more properly a susceptibility mapping based on raster with a spatial resolution of 100 meters developed by CIMA. This dataset classifies vegetation into four main categories: grassland/cropland, broadleaf forest, shrubland, and needleleaf forest. Additionally, each vegetation type is further categorized into three susceptibility levels: high, medium, and low, resulting in a total of 12 classes. To maintain consistency with the classification system used for other hazards, only the susceptibility levels (high, medium, low) were considered, reducing the number of categories to three. Using the same methodology applied for seismic hazard assessment, each cultural asset in the database was assigned a hazard value ranging from 1 to 3 based on its spatial location within the susceptibility (Figure 6).

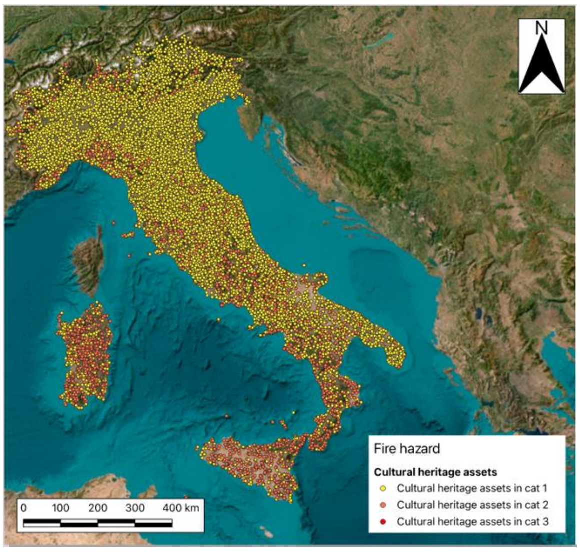

Figure 6. National map showing the wildfire hazard for cultural heritage.

More specifically, the map is generated using a Machine Learning algorithm, specifically a Random Forest Classifier (see Trucchia et al., 2023 for further details on the model). The Machine Learning model classifies each map cell into two categories: either susceptible to wildfire or not. The model then assigns a probability of belonging to the fire class, as a value between 0 and 1. This value is considered indicative of the susceptibility to fire ignition and propagation.

Susceptibility is defined as the probability that a fire will ignite and spread in a specific area, considering predisposing factors such as the area's topography and vegetation type (Leuenberger et al., 2018). It is important to highlight that wildfire susceptibility is driven by predisposing conditions for ignition and propagation and not by transient conditions linked to a specific event - thus representing a static variable.

To perform the classification, the model combines past fire data with predisposing geophysical and climatic variables. The model was trained on a pan-European scale: the geographical scope of the analysis compensates for the limited temporal range of available data, allowing the algorithm to detect the key territorial characteristics that influence fire susceptibility after ignition.

Burned areas across Europe from 2008 to 2022, sourced from the European Forest Fire Information System, EFFIS (EFFIS, 2025), were used to define the class of each cell, indicating whether it experienced a wildfire. Additional geo-topographic variables like slope, aspect (from Multi-Error-Removed Improved Terrain digital elevation model MERIT, Yamazaki et al. 2017) and land cover from the Global Copernicus Land Cover map (Copernicus, 2025) were also included, along with climate indices from the W5E5 dataset as fire-predisposing factors (ISIMIP, 2025).

For the climatic data, some indices were aggregated as 43-year climate averages. All geo-topographic and climate variables used in the model are shown in

Table 2, while Table 9 displays each variable's importance in evaluating susceptibility. This figure highlights that vegetation continuity (i.e., the variable neigh_veg) provides the highest information gain, underscoring the role of vegetation data in determining an area’s susceptibility to fire ignition and spread. The variable importance was evaluated using the Gini impurity index.

Table 2. Predisposing factors used in the Machine Learning wildfire susceptibility model.

	Predisposing factor	Variable name
Topography	Elevation	dem
	Slope	slope
	North side of the slope	north
	South side of the slope	est
Vegetation	Vegetation type	veg
	Tree cover density	TCD
	Vegetation continuity	neigh_veg
Climate	Mean annual relative humidity	RH
	Mean annual temperature (43-years average)	T_average
	Maximum daily temperature (43-years average)	T_max
	Total annual precipitation (43-years average)	Rain
	Mean annual wind speed (43-years average)	Wind
	Maximum annual consecutive dry days (43-years average)	CDD
	Maximum annual consecutive wet days (43-years average)	CWD

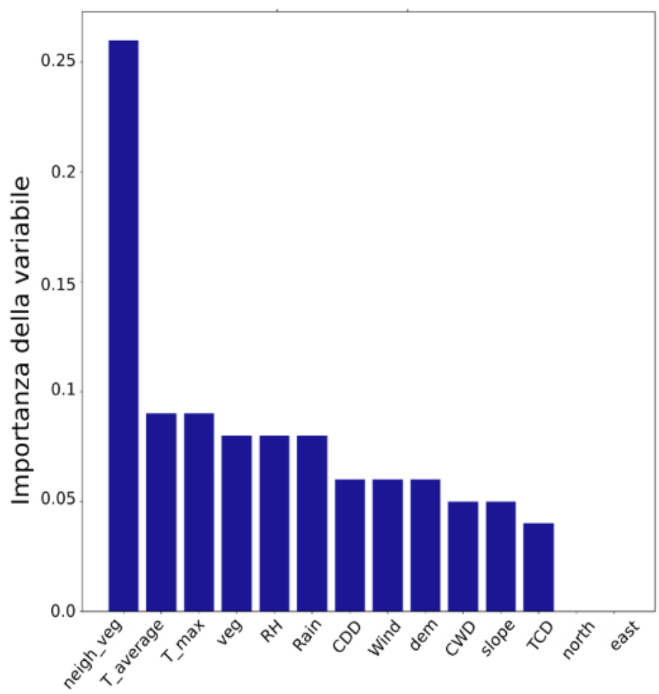

Figure 7. Importance of each variable used by Machine Learning model, defined by Gini's impurity index.

The resulting susceptibility map (see Figure 2-a) is expressed as a continuous value between 0 and 1, where higher values indicate greater likelihood of fire occurrence.

This is also shown in the Figure 8b, where the overall distribution of susceptibility values is compared to those observed during wildfires in Italy from 2007 to 2023 (data source: national inventory shared by Italian Civil Protection Department to CIMA Foundation for research purposes) - a clear distinction is visible between these distributions. Analyzing susceptibility values across different fire size classes (Figure 8b) reveals that small fires (burned area < 1 ha) are mostly associated with low susceptibility values, while large fires (>100 ha and >1000 ha) are statistically linked to high susceptibility values. This analysis shows the informational value of the susceptibility map, as it enables identification of areas where territorial conditions may promote the spread of large-scale fires.

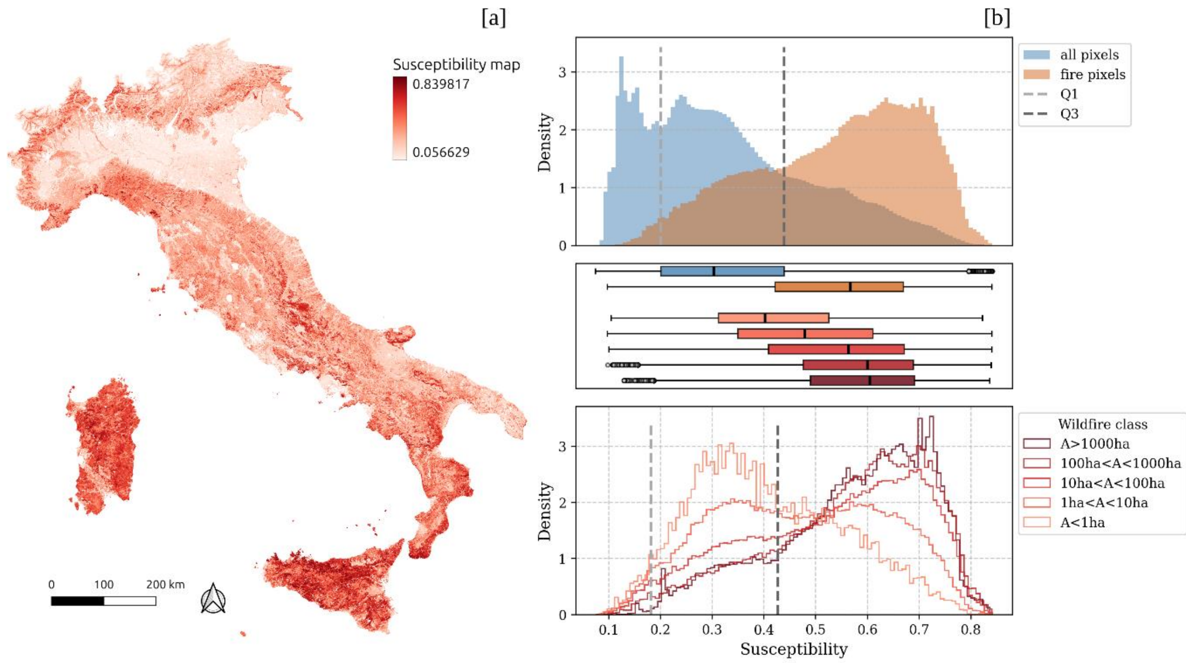

Figure 8. In [a], the susceptibility map for Italy; in [b], the distribution on susceptibility values in wildfires location, compared to the overall distribution (upper plot) and divided by wildfire extension classes (lower plot).

From the continuous susceptibility map, three classes (low, medium, high) were defined based on the 25th and 75th percentiles. These quantiles were calculated at the national level to identify areas with lower and higher susceptibility. Figure 9 shows the distribution of these three classes nationwide, and the percentage of each class affected by wildfires (2007–2023). Results show a strong imbalance: while the high-susceptibility class covers only 25% of the national territory, it includes 10% of burned areas - indicating this area's high fire risk. In contrast, medium and low susceptibility classes show a drastically reduced propensity for fire spread. This confirms the value of using the susceptibility map in RISICO to highlight areas of significant wildfire risk.

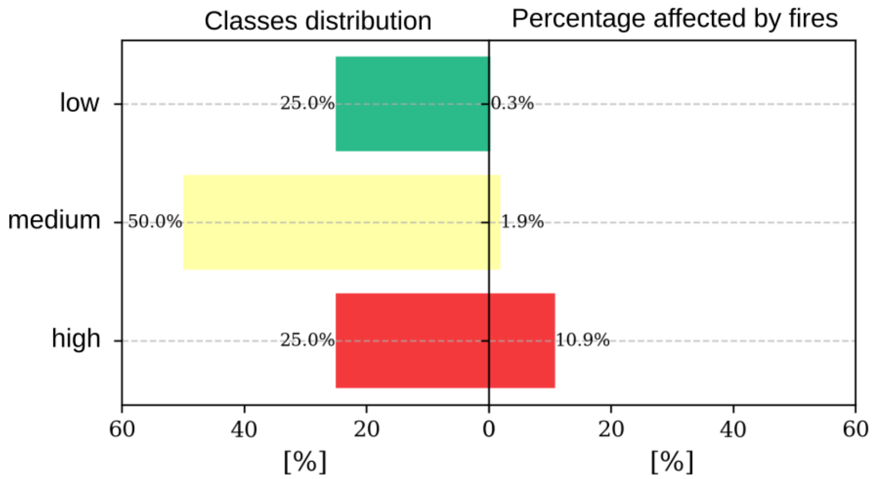

Figure 9. Percentage of coverage of each susceptibility class at national level with respect to the percentage of each class affected by wildfires.

2.4 Vulnerability

Each of the 30 classifications defined in Table 1 was evaluated for each type of risk in relation to its intrinsic vulnerability. As a result, for each class vulnerability was assessed based on the type of risk, assigning a value on a five-class scale (Low, Medium Low, Medium, High and Very High) (Table 3). This coding allowed for the attribution of a vulnerability value ranging from 1 (VL) to 5 (VH) to each element in the database. The classification was based on the structural and functional characteristics; where available, assignments were made starting from scientific literature, otherwise they were based on expert judgement. To validate such assessment, Table 3 has been discussed at the RETURN inter-spoke meeting held in Florence on 13 November 2024 and has been presented at EGU 2025 in Vienna (Intrieri et al., 2025). Assets without a specified typology were excluded from the assessment, resulting in a null value for vulnerability in those cases, therefore the study at the national scale has been done on the 155,076 (83.5%) assets with an assigned typology.

Table 3. Vulnerability matrix for flood (FL), earthquake (EQ), landslide (LS), and wildfire (WF) risks assigned to each class (ranging from 1A to 6E, see Table 1). The possible vulnerability values are very low (VL), low (L), medium (M), high (H) and very high (VH).

		Tall				Equidimensional				Small				Subterranean				Wide			
		A				B				C				D				E			
		FL	EQ	LS	WF	FL	EQ	LS	WF	FL	EQ	LS	WF	FL	EQ	LS	WF	FL	EQ	LS	WF
Buildings potentially containing valuable items	1	H	VH	VH	H	VH	H	VH	H	VH	M	VH	VH	VH	L	L	L	VH	VH	VH	H
Defensive Structures	2	VL	VH	M	M	VL	M	M	M	L	L	H	M	L	VL	L	L	L	H	M	M

Civil buildings and artifacts	3	M	VH	VH	H	H	M	H	H	VH	L	VH	VH	VH	VL	L	L	VH	H	H	H
Infrastructure	4	L	H	H	M	M	L	L	H	H	VL	M	H	H	VL	VL	L	H	M	L	H
Monuments, remains, and archaeological areas	5	VL	L	M	H	L	VL	L	H	M	VL	VL	M	M	VL	VL	L	M	L	L	H
Open spaces, landscapes and associated artifacts, natural monuments	6	L	L	L	H	M	VL	VL	H	H	VL	L	H	H	VL	VL	L	H	L	VL	VH

2.4.1 Landslide vulnerability

In the case of landslides, tall buildings containing valuable objects were classified as Very High vulnerability, as their height increases susceptibility to structural failure and the presence of valuable artifacts amplifies potential damage. On the other hand, low-rise open spaces were generally assigned lower landslide vulnerability values, as they are less prone to collapse and typically contain fewer movable assets at risk (Figure 10).

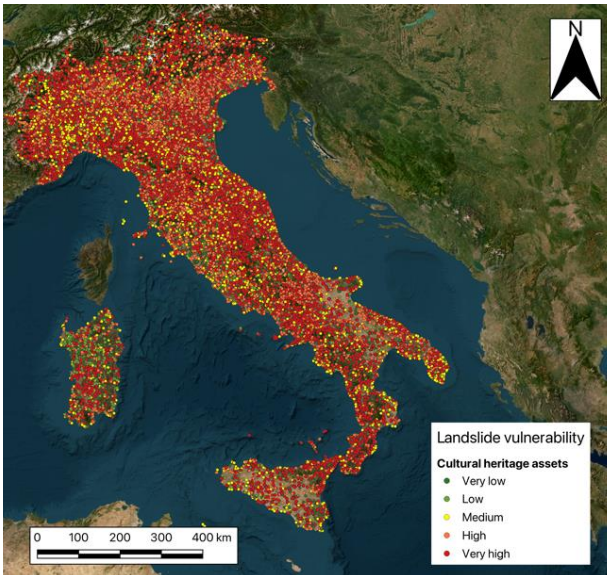

Figure 10. National map showing the landslide vulnerability of cultural heritage.

2.4.2 Flood vulnerability

Concerning floods, the vulnerability of cultural heritage (Figure 11) has been classified based on a taxonomy inspired by existing works on large scale flood risk assessments (Figueiredo et al., 2020; Arrighi et al., 2023; Garrote et al., 2020) that typically identify in cultural buildings with potential high finishing levels, decorations and artworks the highest degree of damage, i.e., religious buildings and museums. Another relevant geometric aspect is the position with respect to the ground and the surface extent that make underground objects or one-story buildings with large footprint more vulnerable than the others.

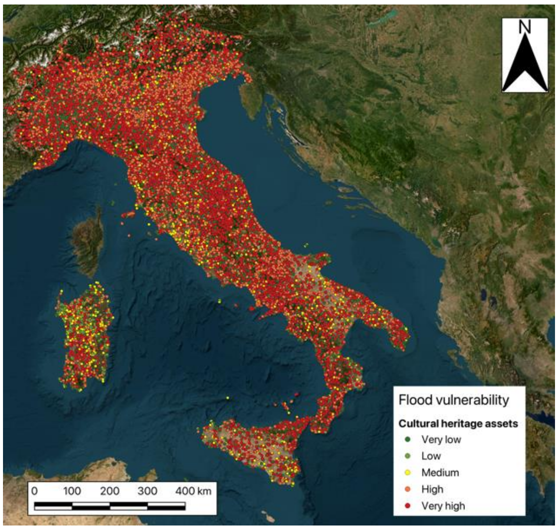

Figure 11. National map showing the flood vulnerability of cultural heritage.

2.4.3 Earthquake vulnerability

Concerning the earthquake vulnerability, the assessment started from previous research (Lagomarsino et al., 2004) that defines monumental buildings typology that are in part overlapping with the ones proposed in Table 1. These values have been firstly normalized within 0 and 1 and then associated to the five vulnerability classes according to the ranges: low (0-0.2); medium-low (0.2-0.4); medium (0.4-0.6); medium-high (0.6-0.8); high (0.8-1) (see Table 4).

Table 4. The building typologies from Lagomarsino et al., 2004 listed within the assumed vulnerability classification.

Typology	Vulnerability class
Arch bridges	Medium-low
Castes	Medium-high
Churches	High
Columns	Medium
Monasteries	High
Mosques	high
Obelisks	Medium
Palaces	Medium-high
Temples	Medium
Towers	High
Triliths	Medium
Triumphal arches	Medium

The typologies for which the literature provides the vulnerability indexes (Table 4) have been imported in the taxonomy matrix as shown in Table 5. The remaining classes have been defined through expert judgment (Table 1) to obtain the vulnerability map (Figure 12).

Table 5. Set of the vulnerability matrix fixing the elements coming from the literature.

		Tall	Equidimensional	Small	Subterranean	Wide
		A	B	C	D	E
Buildings potentially containing valuable items	1	Churches, mosques				
Defensive Structures	2	Towers	Castles			
Civil buildings and artifacts	3	Monastery, Palace		EMS98		
Infrastructure	4		Arch bridges			
Monuments, remains, and archaeological areas	5	Column, Obelisk, Triumphal arches		Temples, Trilite	Trilite	
Open spaces, landscapes and associated artifacts, natural monuments	6					

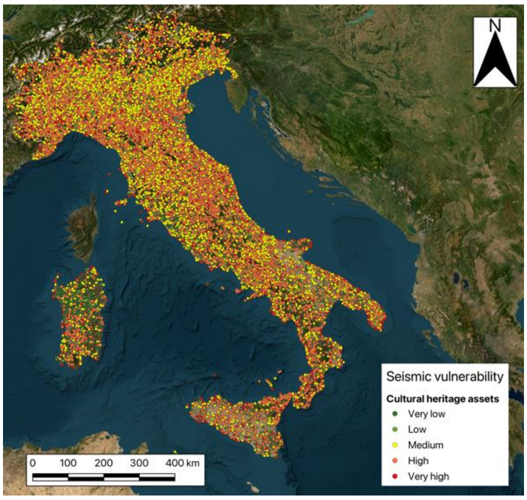

Figure 12. National map showing the seismic vulnerability of cultural heritage.

2.4.4 Wildfire vulnerability

Finally, the vulnerability assessment for wildfire risk follows an expert judgement approach (Table 3). Given the distinct nature of fire-related damages, the classification of vulnerability levels differs from those applied to other hazards (Figure 13).

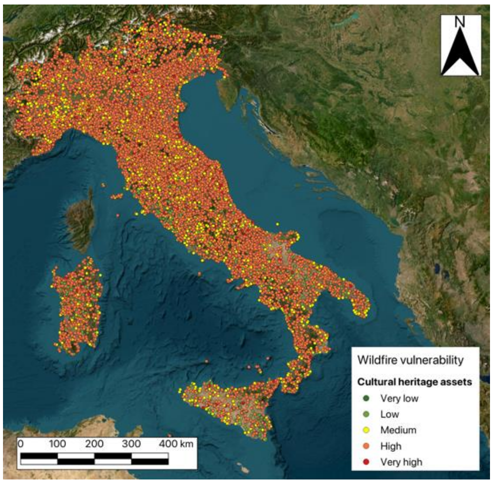

Figure 13. National map showing the wildfire vulnerability of cultural heritage.

2.5 Exposure

Exposure was evaluated based on the level of cultural interest with reference to the four classifications provided in the database (section 2.1): recognized as CH, not still evaluated, under evaluation, of no cultural interest. Assigning 1 and 0 respectively to the first and latter classes, the two remaining classes could have been assigned an intermediate value by default (0.5) or a weighted value based on the probability that a CH under evaluation or to be evaluated will end up in the "recognized as CH" or in the "of no cultural interest" classes. Since only 65 assets (0.04%) were classified as not of cultural interest, it was deemed reasonable to assign an exposure value of 1 to all other assets. This approach is justified by the fact that, generally, the vast majority of assets undergoing verification are ultimately classified as culturally significant. As a result, even assets currently under review have been assigned an exposure value of 1, in line with those already recognized as culturally valuable. Consequently, when mapped, the exposure assessment effectively encompasses the entire database of cultural assets (Figure 14). This approach is applied consistently across all four considered types of risk.

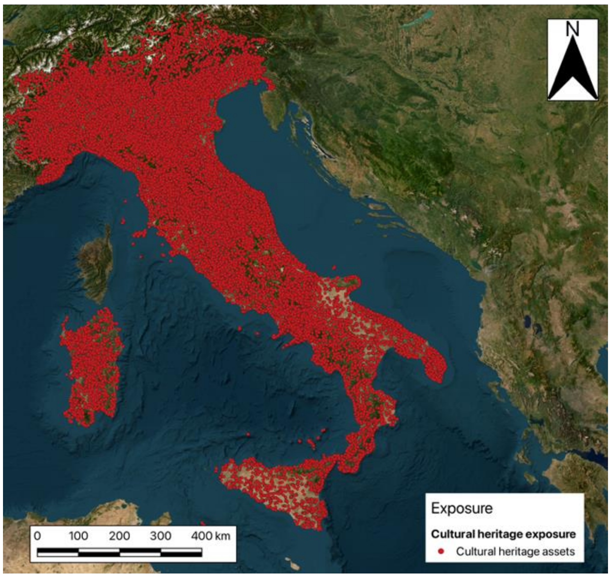

Figure 14. National map of the elements at risk.

2.6 Risk

The risk assessment was conducted following the risk equation outlined in section 1. Specifically, for each cultural asset, the values of H (hazard), V (vulnerability), and E (exposure) were multiplied to obtain a comprehensive risk value. This process was carried out within a GIS environment using the Field Calculator, where the product of these variables—derived from the spatial selection process—was computed. The final output consists of a field containing the total risk value for each asset. To enhance the representativeness and usability of the final risk assessment, data were aggregated at the municipal scale. This was achieved by summing the individual risk values of every asset within each municipality, using administrative boundaries as the spatial reference. The same methodology was applied to all four considered hazards, ensuring consistency in the analysis.

For the cartographic representation of the final risk values, municipalities were classified into five categories (very high, high, medium, low, and very low risk) in addition to a null category for areas with no risk (Figure 15 and Figure 16). Notably, the earthquake risk is ubiquitous with the exception of Sardinia region, so in continental Italy H for earthquakes is never 0; the reason why some municipalities have 0 risk is that they do not contain any cultural heritage, according to the Ministry database.

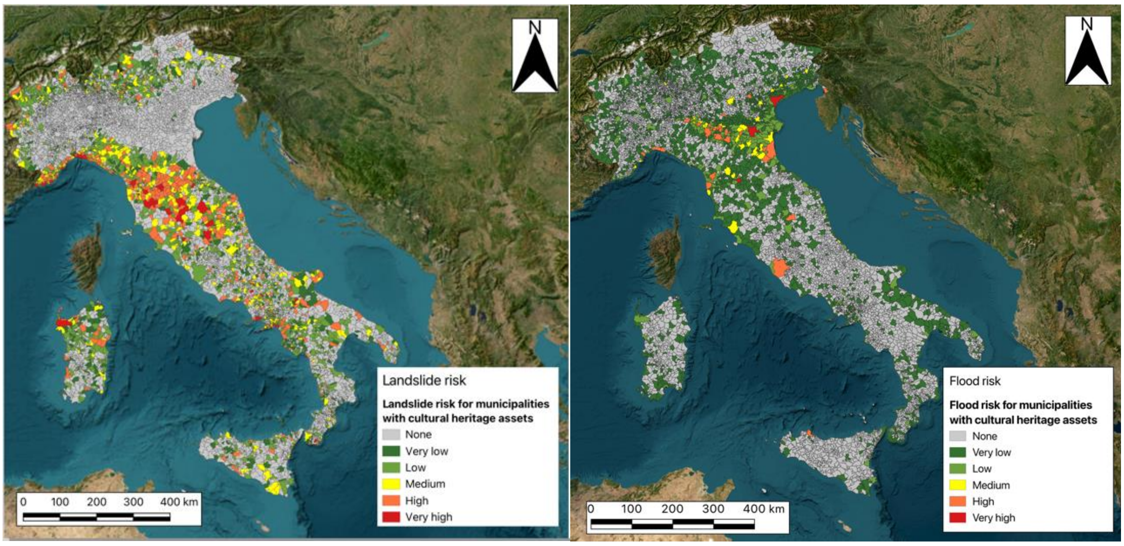

Figure 15. National map of landslide risk (left) and flood risk (right).

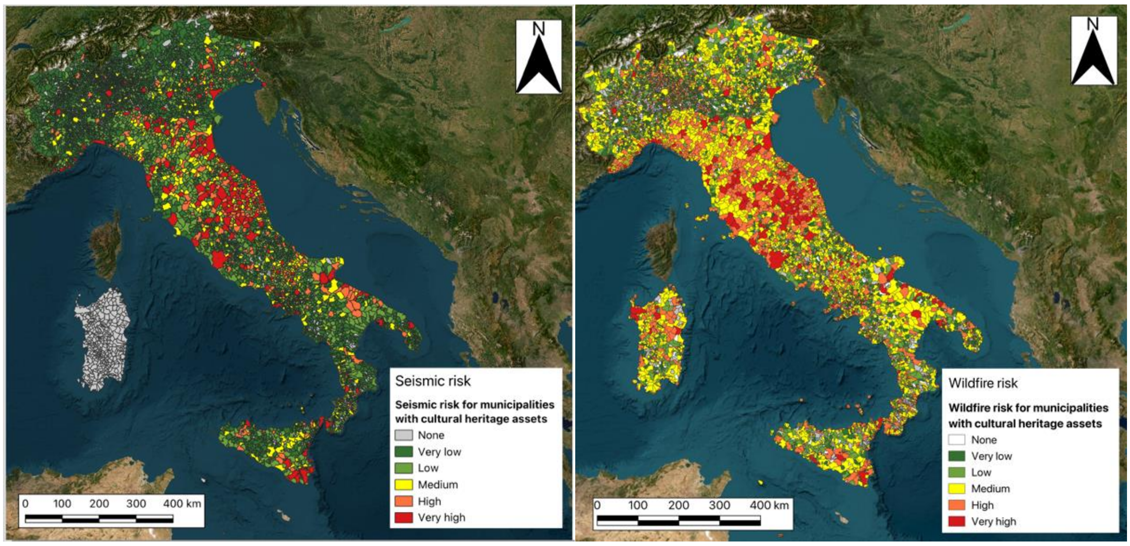

Figure 16. National map of seismic risk (left) and wildfire risk (right).

Before proceeding with the description of the risk categorization, a visualization of the spatial distribution of cultural assets across the Italian territory was carried out. For this purpose, a density map (heatmap) with a 10 km radius was produced, in order to highlight clusters of cultural assets within limited areas, as shown in Figure 17a. In addition, the number of assets was calculated for each municipality, as illustrated in Figure 17b.

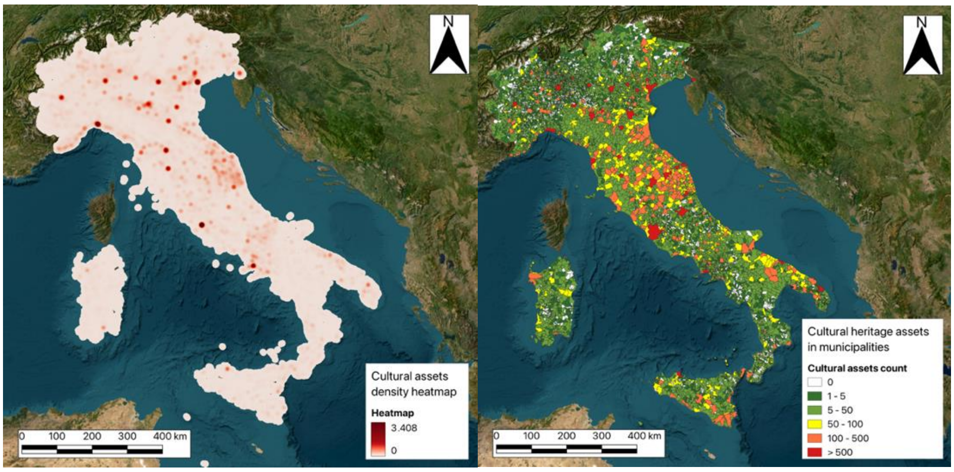

Figure 17. Heatmap of asset density calculated with a 10 km radius (left) and map of the number of assets per municipality (right).

The images clearly show that the spatial distribution of cultural assets in Italy is not homogeneous, but rather tends to concentrate in large cities and historically significant centers. This distribution plays a crucial role in the risk classification process, since both the density and the total number of assets significantly affect the calculation of the risk value (R). For this reason, the density of assets exposed to risk was calculated within each municipality, with the results represented on a scale from 0 to 1, defined as:

$$D = \frac{number\ of\ assets\ at\ risk}{total\ number\ of\ assets}$$

This value makes it possible to highlight the proportion of assets actually exposed compared to the total.

Risk classes are defined based on the value of R, calculated as H × V × E. The classification was designed to represent the data as meaningfully as possible and to ensure a balanced distribution of values across classes.

The use of logarithmic or geometric progressions as separation criteria resulted in an excessive concentration of municipalities in the Very High class, thereby generating an imbalance among the different categories. To overcome this issue, new thresholds were specifically defined for each phenomenon under analysis.

In the overall calculation of R, the values obtained for the four hazards showed different orders of magnitude (as described in the following sections). This disparity could lead to a disproportionate influence of certain hazards over others in the multi-hazard assessment. In other words, without normalization, hazards with higher absolute values would carry greater weight in the overall classification, regardless of their relative significance.

To ensure a consistent comparison across hazards and a balanced evaluation of multi-hazard risk, a normalization procedure was introduced using the following indicators:

- $\boldsymbol{R_{norm}} = \left(\frac{R}{R_{max}}\right) * 1000$
- $\boldsymbol{R_{sup}} = \left(\frac{R_{norm}}{Area\ municipality\ (km^2)}\right)$
- $\boldsymbol{R_{beni}} = \left(\frac{R_{norm}}{n^{\circ}\ exposed\ assets}\right)$

Where R represents the risk value for the municipality, R_{max} is the maximum R value among all municipalities, R_{norm} allows scaling values onto a common scale from 0 to 1000, while R_{sup} enables the assessment of normalized risk relative to territorial extent, highlighting potential concentrations of exposed assets in restricted areas. R_{beni} normalizes the R value with respect to the total number of assets.

The class thresholds for R may vary depending on the specific distribution of the data, whereas for R_{norm} and R_{sup} they are uniform across all four hazards (Table 6), ensuring consistency in classification. With regard to R_{beni}, as with the non-normalized R, the classes were defined on a case-by-case basis.

Table 6. Risk classes for R_{norm} and R_{sup}.

Classes R_{norm}		Classes R_{sup}	
Very low	0 – 1	Very low	0 – 0,1
Low	1 – 5	Low	0,1 – 0,5
Medium	5 – 10	Medium	0,5 – 1
High	10 – 100	High	1 – 5
Very High	100 - 1000	Very High	> 5

For landslide risk, the density of assets at risk within each municipality was calculated, as shown in Figure 18.

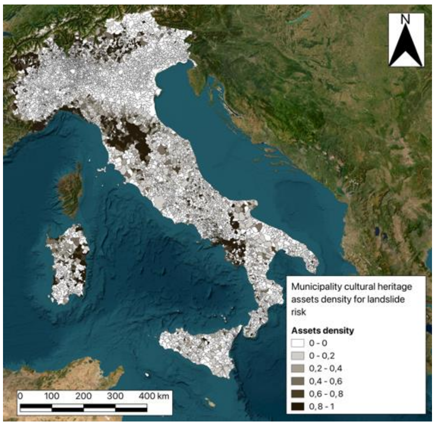

Figure 18. Density of assets at landslide risk calculated within municipalities.

For the classification of non-normalized R and R_{beni}, the classes shown in Table 7 were selected to best represent the data frequency illustrated in Figure 19a, b, c, and d. The results are shown in Figure 4a, b, c, and d.

Table 7. Classes for non-normalized landslide R and R_{beni}.

Classes R landslide		Classes R_{beni} landslide	
Very low	1 – 10	Very low	0 – 0,1
Low	10 – 50	Low	0,1 – 0,5
Medium	50 – 100	Medium	0,5 – 1
High	100 – 500	High	1 – 1,5
Very high	> 500	Very high	> 1,5

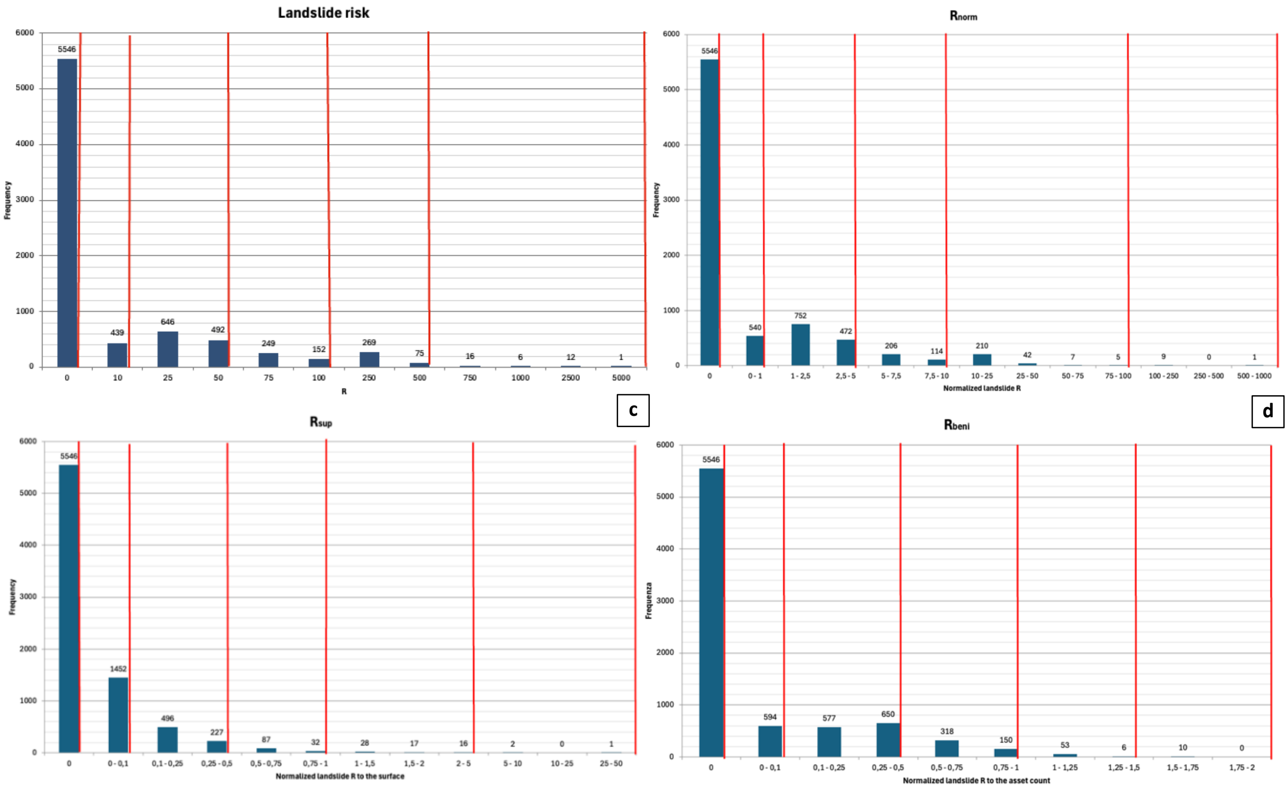

Figure 19. Frequency distribution of landslide risk values R (a), R_{norm} (b), R_{sup} (c), and R_{beni} (d) with class separation.

In the Very High class there are 35 municipalities for R, 10 for R_{norm}, 1 for R_{sup}, and 10 for R_{beni}.

The same procedure has been applied to flood, earthquake and wildfire risks as well.

R is not normalized, which means that there is no maximum value for R. Depending on the type of risk, the possible range of R values is very variable. For example, the earthquake risk has municipalities with many exposed assets. When the risk value of each individual asset is summed up to calculate the R for that municipality, the result can be as high as 50.000, while the wildfire risk reaches as high as 5.000. Without normalization, this would produce a bias that gives a higher weight to the earthquake risk. For this reason, R has not been considered suitable for further analyses, such as multi-risk calculation.

This issue is solved using R_{norm} that normalizes the risk values for each type of risk with respect to its maximum value so that every risk has the same potential range (e.g. from 0 to 1).

In R_{sup}, the extension of a municipality does not effect its risk, so that larger or smaller municipalities are not biased; however it is still affected by the density of assets, since the risk value is obtained by summing the single risk values for each asset, therefore the total number of assets influences the final R_{sup} value, according to the following equation:

$$R_{sup} = \frac{\sum R_{asset}}{area} = \frac{\bar{R}_{asset} \cdot number\ of\ assets}{area} = \bar{R}_{asset} \frac{number\ of\ assets}{area} = \bar{R}_{asset} \cdot asset\ density$$

with $\bar{R}_{asset} = \frac{\sum R_{asset}}{number\ of\ assets}$ being the average risk value of each asset in a single municipality. R_{sup} is useful if the intrinsic risk of a municipality is deemed of interest and if the density of assets has to be factored into, which puts at the same level large and small municipalities if both are relatively rich with cultural heritage.

R_{beni} would be identical to R_{sup} in the ideal hypothesis that the assets are homogenously distributed within the national territory. On the other hand, R_{beni} produced maps that were very similar to the corresponding hazard and risk maps because the equation above shows that the result would only be dependent from the $\bar{R}_{asset}$:

$$R_{beni} = \frac{\sum R_{asset}}{number\ of\ assets} = \frac{\bar{R}_{asset} \cdot number\ of\ assets}{number\ of\ assets} = \bar{R}_{asset}$$

Since the exposure has been assumed 1 for each asset at the national level, this means that R_{beni} Only depends from V and H that for the earthquake risk are strongly correlated, resulting in an as much correlated R_{beni} earthquake map. For this reason, R_{beni} has not been considered suitable for further analyses, such as multi-risk calculation.

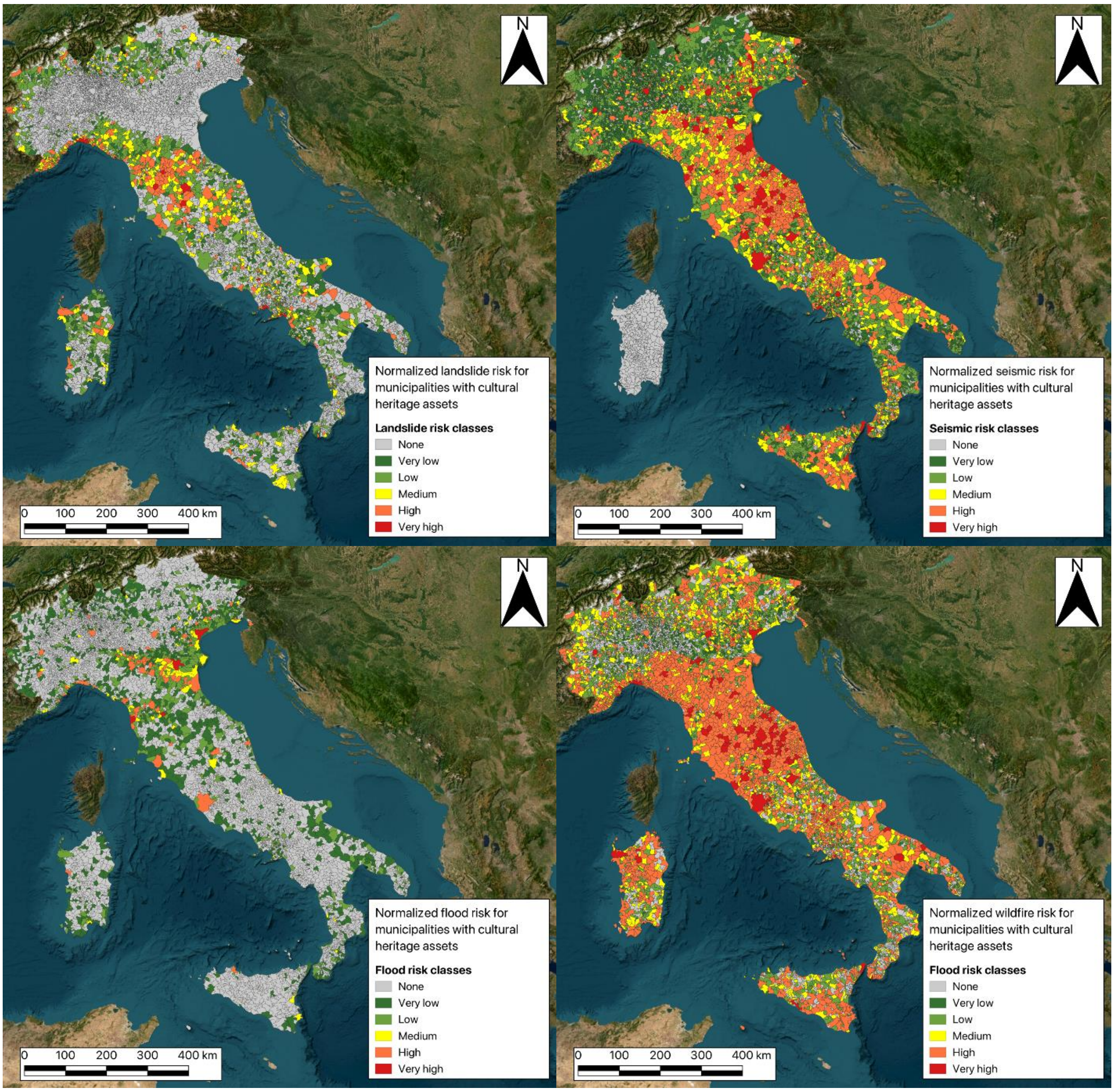

Figure 20. Risk maps using R_{norm} for landslide, earthquake, flood and wildfire risks.

2.7 Multi-risk at national scale

The methodology used for multi-risk classification assigns an overall risk class to each municipality based on the individual risk classes for landslides, floods, wildfires, and earthquakes. R_{norm} has been used instead of using absolute risk values (R), which can vary greatly between hazards. The values have been then classified and subdivided into 5 classes (very low, low, medium, high, very high). This subdivision into classes is not linear but has been done using natural breaks and then adjusted to include in the highest risk class only a small number of municipalities; this subdivision can be arranged according to representation needs (Figure 21).

Then the multi-risk classification follows logical criteria that count if and how many single risks fall in a certain class. The aim is to avoid instances where the multi-risk class designation might be due to a single anomalous risk value, instead giving weight to the compresence of multiple risks. To do so, each risk class has been attributed a value from 1 (very low) to 5 (very high).

Then, the multi-risk classes have been assigned according to the following classification criteria:

- Very high ≥ 15
- High ≥ 11
- Medium ≥ 9
- Low ≥ 6
- Very low ≤ 5.

This approach avoids distortions from normalizing values of different magnitudes and treats all risks equally. It also enhances comparability between municipalities and provides a more intuitive understanding of risk distribution, yielding balanced and realistic results. This map (Figure 21) provides a tool for policy makers and highlights in red the municipalities that have many assets exposed to high levels of several risks. A modified version of this map can be obtained by normalizing the risk values on the surface area or on the number of cultural heritage assets of each municipality (as explained in the previous section) and is shown in Figure 21 (right).

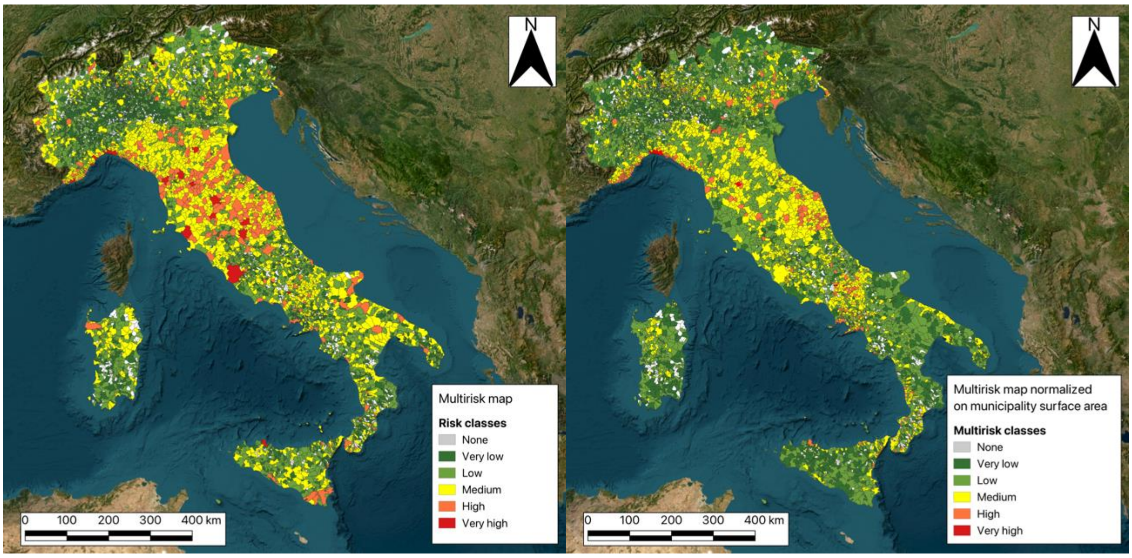

Figure 21. Spatial map of municipalities by multi-hazard risk (right).

3 Regional scale

The Sardinia Region case study represents an intermediate scale of analysis, between the national and urban applications. The focus is on a specific regional context, characterized by the unique presence of Nuragic heritage, an ensemble of prehistoric stone structures distributed across the island and recognized for their outstanding cultural significance.

3.1 Cultural Heritage Database

The Sardinia case study is based on a dedicated cultural heritage database focusing on Pre-Nuragic and Nuragic monuments, which constitute the most distinctive archaeological assets of the island. The database was designed in GIS format (vector shapefile) to enable systematic monitoring and risk assessment. Two open-access inventories were integrated:

- *SardegnArcheologica*, an official initiative cataloguing and georeferencing archaeological sites with particular emphasis on nuraghe.
- *Nurnet – La rete dei Nuraghi*, a participatory platform documenting and promoting Sardinia's prehistoric heritage, where contributions are continually updated and reviewed by experts.

The harmonization process followed several GIS-based operations:

1. Georeferencing and integration of the two inventories, with the removal of duplicate entries.
2. Standardization of attributes into a common structure (site name, typology, chronology, geometry, materials).
3. Linking with ancillary data, including regional lithological maps from the Sardinia GeoNetwork, to assign construction materials when direct descriptions were unavailable. These were used as a proxy for construction materials, under the assumption that prehistoric builders relied on locally available stone resources.
4. Database formatting into a vector shapefile, enabling spatial overlay with hazard and vulnerability layers for multi-risk assessment.

The final dataset comprises 7335 monuments, spatially distributed across the island and enriched with attributes describing typology, geometry, chronology, and (where possible) construction materials. Although the use of lithology as a proxy introduces some uncertainty, it provides a consistent basis for both vulnerability assessment and long-term monitoring of the Nuragic network. Table 8 shows the percentage of coverage of various types of structures, while Figure 22 displays the Sardinian map with the completed regional database and the associated pie chart.

Table 8. Percentage of coverage of the various types of structures.

Megalithic circles	2.1%
Dolmen	1.3%
Domus de Janas	11.0%
Springs and sacred wells	4.2%
Cave	0.4%
Menhir	1.8%
Nuraghe - corridor	6.2%
Nuraghe - complex	15.1%
Nuraghe - complex mixed	0.9%

Nuraghe - singletower	35.0%
Sanctuary	0.4%
Giants' tomb	17.0%
Nuragic Village	4.4%
Shelter	0.2%

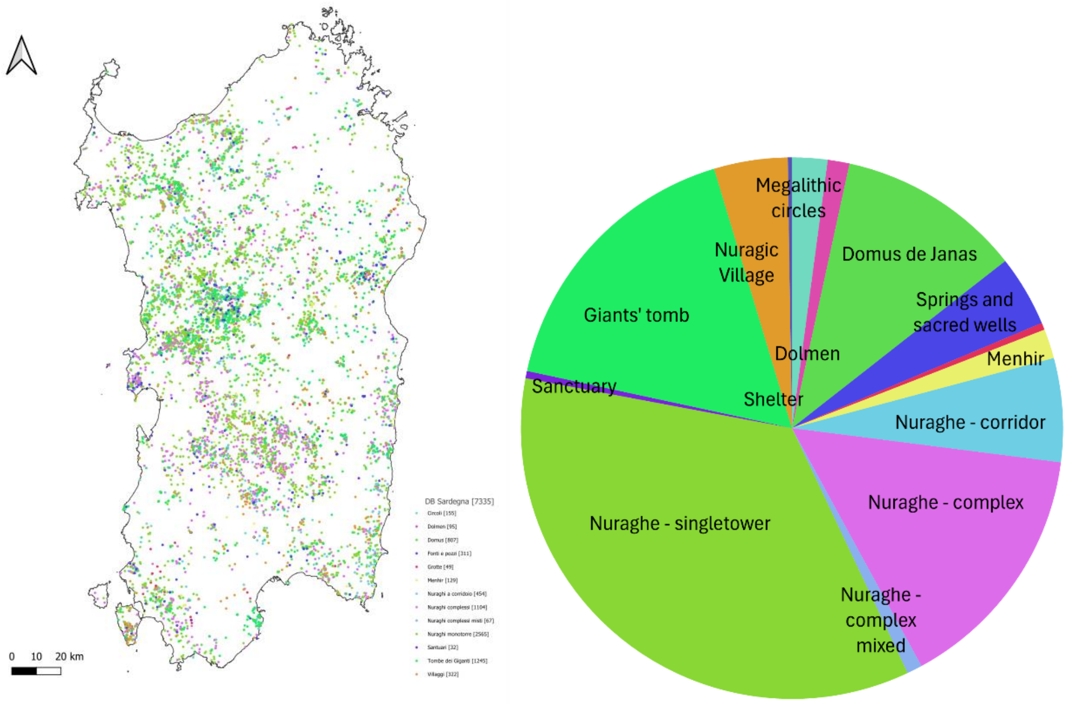

Figure 22. Completed regional database with the building typologies; pie chart.

3.2 Typological classification

The monuments included in the Sardinia-scale database belong to the Pre-Nuragic and Nuragic cultural phases, covering a chronological span from the Neolithic to the Early Iron Age. Although all assets fall under the general class Monuments, remains and archaeological areas (Category 5), they present a remarkable diversity in terms of function, morphology, and construction techniques.

For analytical purposes, the classification adopted a dual approach, combining typological and geometric criteria:

1. **Typological classification**. 13 main categories were identified based on archaeological literature and regional inventories. Each typology was linked, where possible, to its chronological period.
2. **Geometrical classification.** To capture the structural configuration of monuments and their potential response to hazards, each site was also assigned to a geometric class according to the height-to-width ratio of its main structure.

Table 9. Classification of the selected building typologies in terms of geometry and historical period.

ID	Building Typology	Geometry	Period
5.1	Nuraghe – corridor	Equidimensional (B)	1700-1350 A.C., Middle Bronze Age
5.2	Nuraghe – singletower	Equidimensional (B)	1500-1350 B.C.

5.3	Nuraghe - complex	Equidimensional (B)	
5.4	Giants' tomb	Wide (E)	Bronze Age
5.5	Sacred weels	Subterranean (D)	Bronze Age, early Iron Age
5.6	Domus de Janas	Subterranean (D)	1800-1600 B.C., Middle Neolithic
5.7	Cave	Subterranean (D)	From 5th to the end of the 3rd millennium A.C.
5.8	Shelter	Small (C)	From 5th to the end of the 3rd millennium A.C.
5.9	Menhir	Tall (A)	From Neolithic to Copper Age
5.10	Dolmen	Tall (A)	From Neolithic to Copper Age
5.11	Megalithic circles	Tall (A)	Middle Neolithic
5.12	Sanctuary	Wide (E)	
5.13	Nuragic Village	Wide (E)	1350 B.C. – 950 B.C.

In addition, the classification incorporated information on construction materials, derived indirectly from the regional lithological map. When monuments fell within lithological polygons of excluded classes, a GIS–Python procedure was applied to evaluate neighbouring polygons and assign the most probable lithology based on spatial proximity. This approach was necessary because direct descriptions of materials are not systematically available in the inventories, and it assumes that prehistoric builders relied primarily on locally available stone resources. Although this method introduces some uncertainty, it ensures a consistent proxy for subsequent vulnerability and risk assessments. This method, followed by grouping into macro-categories, allowed the systematic integration of construction materials into the database (Figure 23), ensuring consistency for subsequent vulnerability and risk analyses

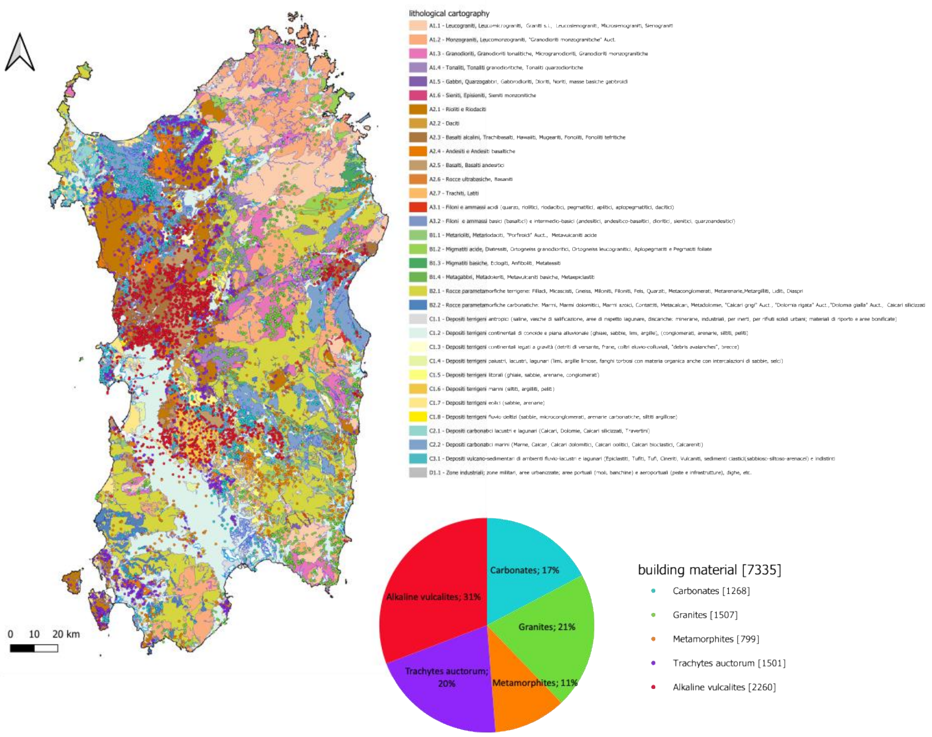

Figure 23. Completed regional database with the construction materials; pie chart depicting materials percentages.

3.3 Hazard

3.3.1 Landslide Hazard

The hazard analysis was based on the official maps sourced from the PAI (Piano Stralcio per l'Assetto Idrogeologico) (Regione Autonoma della Sardegna, 2006). In particular, the "hydrogeological" map was specifically used to indicate landslide risk exposure (Figure 24). As a preliminary step, the official hazard map was resampled on the monuments' positions, generating an additional field that contained the corresponding official hazard class. Subsequently, the official categories were simplified, providing a numeric and unified classification divided into five classes with equivalent meanings. Following this step, a new field value, H_l was given to each monument.

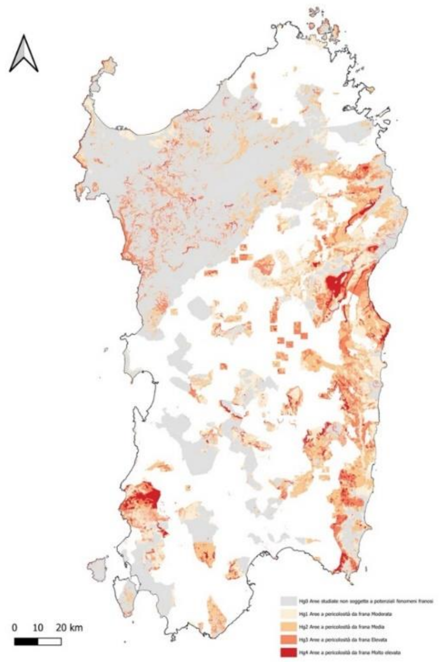

Figure 24. PAI official map for landslides hazard.

3.3.2 Flood Hazard

The hazard analysis was based on the official maps sourced from the PAI (Piano Stralcio per l'Assetto Idrogeologico) (Regione Autonoma della Sardegna. Piano Stralcio di Bacino per l'Assetto Idrogeologico (PAI, 2006; Figure 24). As a preliminary step, the official hazard map was resampled on the monuments' positions, generating an additional field that contained the corresponding official hazard class. Subsequently, the official categories were simplified, providing a numeric and unified classification divided into five classes with equivalent meanings. Following this step, a new field value, H_h was given to each monument.

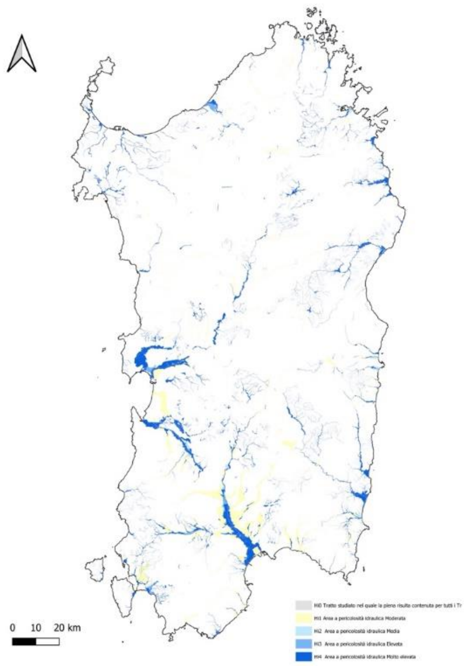

Figure 25. PAI official map for hydraulic hazard.

3.3.3 Earthquake Hazard

Since Sardinia is known to be particularly stable from a seismic point of view (Meletti et al., 2021; Gorshkov et al., 2021; Anselmi et al., 2020), no seismic hazard map was employed, and a constant hazard value, H_s, was applied. A value $H_s = 1$ was assigned to the seismic hazard to indicate the low seismicity in Sardinia while preventing a total underestimation of the issue (without using class 0).

3.3.4 Wildfire Hazard

The Geoportal of the Sardinia region was used to download the wildfire hazard map, given its specificity for the Sardinia region, which particularly suffers from this issue (Salis et al., 2015; Cardil et al., 2014) (Figure 26). As a preliminary step, the official hazard map was resampled on the monuments' positions, generating an additional field that contained the corresponding official hazard class. Subsequently, the official categories were simplified, providing a numeric and unified classification divided into classes with equivalent meanings. For the wildfire hazard, the two classifications are equivalent since the official maps already employed a numeric classification. Following this step, a new field value, H_w was given to each monument.

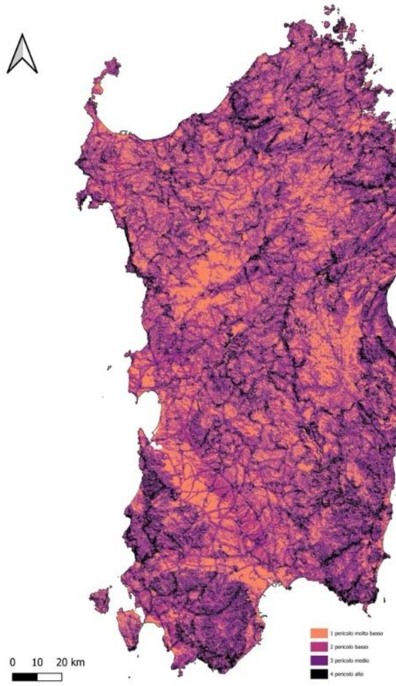

Figure 26. Wildfire Hazard Map from Geoportal of the Sardinia Region (https://www.sardegnageoportale.it/).

3.4 Vulnerability

Vulnerability expresses the potential damage to a structure caused by a hazardous event of given intensity, ranging from 0 (no loss) to 1 (total loss). For the Sardinian case study, this concept was applied to prehistoric and Nuragic monuments (Neolithic–Iron Age), composed of stone blocks arranged in characteristic geometries.

Two complementary mechanisms were considered:

- Geometric vulnerability, related to the overall stability of structures, depending on height-to-width ratio and position relative to the topographic surface. Five classes were defined: equidimensional, wide, tall, subterranean, and small.
- Material vulnerability, determined by the resistance of stone blocks to external stresses. Mechanical resistance refers to the capacity to remain intact without cracking or breaking; chemical resistance indicates the ability to withstand weathering and alteration.

The main lithologies used (granitoids, basalts, trachytes, metamorphic and carbonate rocks) were evaluated according to these criteria. Hazards such as floods, earthquakes, and landslides primarily affect the overall geometry, while wildfires directly impact the physical integrity of blocks through thermal degradation.

On this basis, vulnerability values were assigned on a five-level scale (1–5), integrating structural geometry, block stability, and material integrity. Level 1 corresponds to no significant effects, while level 5 indicates collapse, fragmentation of blocks, and irreversible loss of material, making recovery impossible.

3.4.1 Landslide vulnerability

Landslide vulnerability was assessed by combining geometric configuration and material resistance. Geometric vulnerability (Table 1. The elements at risk have been reclassified from 1A to 6E according to their geometry and category. reflects the stability of structural forms: tall and slender monuments (e.g., menhirs, towers) are more prone to overturning and differential movements, while subterranean sites such as domus de Janas or sacred wells are less exposed. Wide and equidimensional structures were classified in intermediate classes.

Material vulnerability (Table 11) was derived from the unconfined compressive strength (UCS) and the Index of Susceptibility to Instability (ISI) calculated from lithological properties. Strong volcanic rocks generally correspond to low vulnerability, whereas carbonate or poorly cemented lithologies show higher susceptibility.

The two dimensions were combined into a five-level scale (very low to very high), ensuring consistency with the multi-hazard framework adopted across scales.

Table 10. Landslide hazard: geometric vulnerability classification of the Pre-Nuragic and Nuragic structures.

Geometric type	**Archeological type**	**Damage Level after Landslide (damage level specification)**	**Geometric vulnerability**
		1 (the structure is not affected by the event and is intact, in a good state of preservation; the blocks do not undergo relative movement)	None (1)
Subterranean **Wide**	Sacred weels Domus de Janas Cave Giants' tomb Sanctuary Nuragic Village	2 (structural elements may undergo relative displacements that do not compromise overall stability)	Low (2)
Equidimensional	Corridor Nuraghe Single tower Nuraghe Complex Nuraghe	3 (structural elements can undergo displacements that challenge the overall stability without leading to the collapse of the structure)	Medium (3)
Small	Rock shelter	4 (the structure undergoes major relative displacements that challenge its geometric structure)	High
Tall	Menhir Dolmen Megalithic circles	5 (the structure undergoes major relative displacements that challenge its geometric structure, and the original blocks have newly formed through-going fractures that generate fragmentation)	Very High

Table 11. Relationship between the UCS values of the lithotypes present in Sardinia, their ISI value and their vulnerability to landslide, flood and earthquake hazards.

	Granitoids	Basalts	"Auctorum" Trachytes	Metamorphic rocks	Carbonate Rocks
UCS [MPa] (Sardinian mean value)	155	115	58	110	100
ISI [%]	84	75	61	74	71
Material vulnerability	Low (2)	Medium (3)	Very High (5)	High (4)	High (4)

3.4.2 Flood vulnerability

Flood vulnerability was defined by the interaction of geometry and material sensitivity to water degradation (Table 12). Subterranean monuments (sacred wells, domus de Janas, caves) were assigned high vulnerability due to infiltration and submersion risks. Wide monuments such as Giant's tombs are also prone to water stagnation. In contrast, tall and massive above-ground structures were generally less affected.

For landslides, floods, and earthquakes, incidental scenarios may cause the collapse or displacement of stone blocks, with consequent degradation from impacts. The vulnerability of blocks is therefore linked to the mechanical strength of their lithology, and the evaluation of material vulnerability to earthquakes follows the same approach adopted for landslides.

Table 12. Flood hazard: geometric vulnerability classification of the Pre-Nuragic and Nuragic structures.

Geometric type	Archeological type	Damage Level after Landslide (damage level specification)	Geometric vulnerability
		1 (the structure is not affected by the event and is intact, in a good state of preservation; the blocks do not undergo relative movement)	None (1)
Equidimensional Tall	Corridor Nuraghe Single tower Nuraghe Complex Nuraghe Menhir Dolmen Megalithic circles	2 (structural elements may undergo relative displacements that do not compromise overall stability)	Low (2)
Wide	Giants' tomb Sanctuary Nuragic Village	3 (structural elements can undergo displacements that challenge the overall stability without leading to the collapse of the structure)	Medium (3)
Subterranean Small	Sacred weels Domus de Janas Cave Rock shelter	4 (the structure undergoes major relative displacements that challenge its geometric structure)	High
		5 (the structure undergoes major relative displacements that challenge its geometric structure, and the original blocks have	Very High

		newly formed through-going fractures that generate fragmentation)	

3.4.3 Earthquake vulnerability

Seismic vulnerability was evaluated by linking geometric configuration to material resistance (Table 13). Tall structures were considered the most vulnerable due to their unfavorable height-to-width ratio and higher susceptibility to seismic accelerations. Equidimensional and wide monuments were placed in intermediate classes, while subterranean structures (domus de Janas, sacred wells, caves) exhibit very low seismic vulnerability because of their embedding in the ground.

Lithological resistance was assessed with the same UCS- and ISI-based criteria adopted for landslides and floods, ensuring comparability. Materials with low cohesion or susceptibility to cracking increase seismic vulnerability, whereas massive volcanic rocks mitigate it.

The final classification integrates geometry and materials into a five-level vulnerability score, aligned with the broader methodological framework.

Table 13. Seismic hazard: geometric vulnerability classification of the Pre-Nuragic and Nuragic structures.

Geometric type	Archeological type	Damage Level after Landslide (damage level specification)	Geometric vulnerability
		1 (the structure is not affected by the event and is intact, in a good state of preservation; the blocks do not undergo relative movement)	None (1)
Subterranean	Sacred weels Domus de Janas Cave	2 (structural elements may undergo relative displacements that do not compromise overall stability)	Low (2)
Wide **Small**	Giants' tomb Sanctuary Nuragic Village Rock shelter	3 (structural elements can undergo displacements that challenge the overall stability without leading to the collapse of the structure)	Medium (3)
Equidimensional	Corridor Nuraghe Single tower Nuraghe Complex Nuraghe	4 (the structure undergoes major relative displacements that challenge its geometric structure)	High
Tall	Menhir Dolmen Megalithic circles	5 (the structure undergoes major relative displacements that challenge its geometric structure, and the original blocks have newly formed through-going fractures that generate fragmentation)	Very High

3.4.4 Wildfire vulnerability

Wildfire vulnerability was assessed by combining geometric characteristics of monuments with the thermal behavior of construction materials. This dual perspective reflects the fact that exposure to fire is not uniform: the way a structure absorbs, resists, or dissipates heat strongly depends on both its shape and its lithological composition.

From the geometric standpoint (Table 14), monuments were classified according to their height-to-width ratio. Tall and slender structures (e.g., menhirs, towers) were considered the most vulnerable, as they are subject to sharp thermal gradients and higher risks of block detachment or collapse when heated unevenly. Wide and equidimensional monuments present intermediate conditions: their bulk provides some protection, but outer elements and architectural discontinuities remain exposed. Subterranean monuments such as domus de Janas or sacred wells were assigned very low wildfire vulnerability, since their embedding in soil and rock shields them almost completely from direct exposure.

Material vulnerability (Table 15) reflects the response of lithologies to high temperatures. Volcanic rocks such as basalts or trachytes are generally resistant, with only surface alterations under fire. In contrast, carbonates and friable sedimentary rocks may undergo cracking, spalling, or loss of cohesion when subjected to prolonged heating. These processes, although localized, can compromise structural stability and accelerate long-term decay.

The integration of geometric and lithological criteria allowed the definition of a five-level vulnerability scale, ranging from very low (subterranean monuments in volcanic rocks) to very high (slender structures in thermally sensitive lithologies).

Table 14. Wildfire hazard: geometric vulnerability classification of the Pre-Nuragic and Nuragic structures.

Geometric type	**Archeological type**	**Damage Level after Fire (damage level specification)**	**Geometric vulnerability**
Subterranean	Sacred wheels Domus de Janas Cave	1 (the block material is not exposed: the structure is not changed)	None (1)
Wide Small	Giants' tomb Sanctuary Nuragic Village Shelter	2 (the block material is exposed – the blocks are small and suffer limited damage)	Low (2)
Equidimensional	Corridor Nuraghe Single tower Nuraghe Complex Nuraghe	3 (the block material is exposed – the blocks are large and suffer significant damage – the structure does not lose geometric integrity)	Medium (3)
Tall	Menhir Dolmen Megalithic circles	4 (the block material is exposed – the structures are monolithic; the blocks are cracked and fractured into smaller pieces, and the structure loses geometric integrity)	High (4)
-		5 (the block material is exposed – the blocks are cracked and fractured into smaller pieces, the structure loses geometric integrity – the material of the blocks is disintegrated)	Very High (5)

Table 15. Wildfire hazard: vulnerability classification of the materials used for the construction of Pre-Nuragic and Nuragic structures.

Material Type	Damage Level after Fire (damage level specification)	Material Vulnerability
	1 (lithotype undergoes color changes but no form of degradation)	None (1)
Basalts	2 (lithotype undergoes color changes and degradation pathologies such as slight fissuring (microcracking))	Low (2)
Granitoids **Metamorphic rocks** **Trachytes "auctorum"**	3 (lithotype undergoes color changes and degradation pathologies such as fissuring and detachment of surface fragments)	Medium (3)
	4 (lithotype with severe compromise of material consistency/composition)	High (4)
Carbonate rocks	5 (lithotype loses even material consistency, becoming totally inefficient and unrecoverable)	Very High (5)

3.5 Risk

The risk analysis follows the same approach for all selected hazards. For simplicity, it is reported at the beginning of this chapter, while the resulting maps will be shown in their respective chapters. Having completed the monuments' database with the associated classes of vulnerabilities and hazard enabled the assessment of the risk R_i, computed as:

$$R_i = H_i \cdot V_{geom,i} \cdot V_{mat,i}$$

Subsequently, a normalization was applied to adjust the final values to the five-level scale, considering the minimum and maximum possible risk values $R_{i,min}$ and $R_{i,max}$:

$$R_{i,min} = 0$$

$$R_{i,max} = H_{i,max} \cdot V_{geom,i,max} \cdot V_{mat,i,max} = 4 \cdot 5 \cdot 5 = 100$$

At this point, the risk value was reclassified according to the criteria outlined in Table 16, which divides values from 1 to 100 into 5 distinct risk classes.

Table 16. Risk classification according to the 5-level scale.

0-20	20-40	40-60	60-80	80-100
1	2	3	4	5
VL	L	M	H	VH

The map reporting landslides risk values associated with each monument considered is shown in Figure 27.

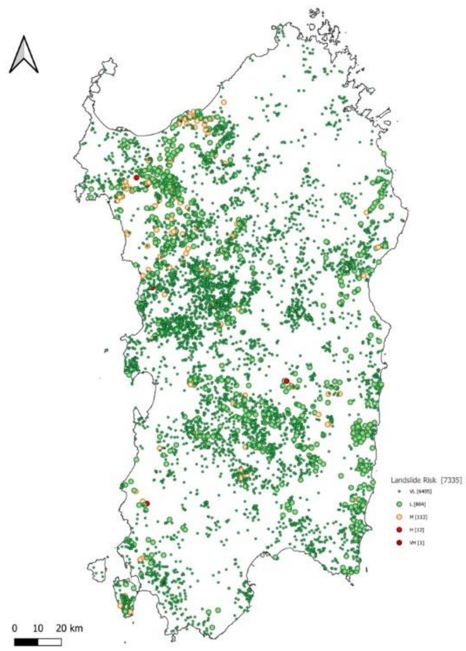

Figure 27. Landslides risk map.

The map reporting flood risk values associated with each considered monument is shown in Figure 28.

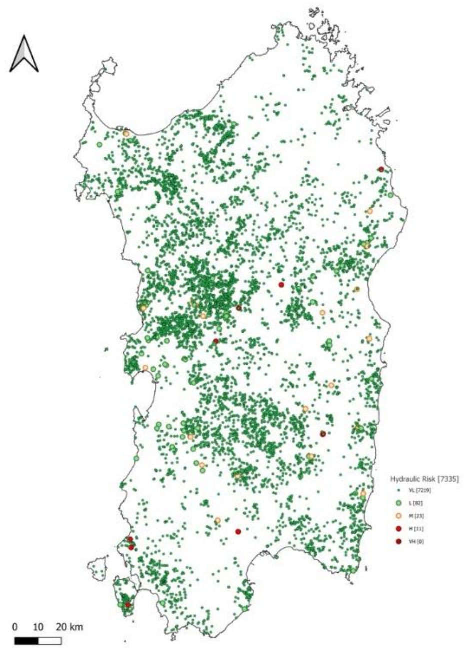

Figure 28. Flood risk map.

The map reporting seismic risk values associated with each considered monument is shown in Figure 29.

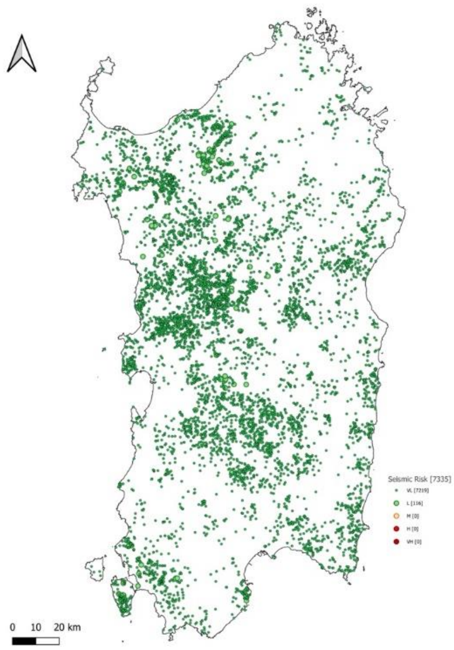

Figure 29. Seismic risk map.

The map reporting wildfire risk values associated with each considered monument is shown in Figure 30.

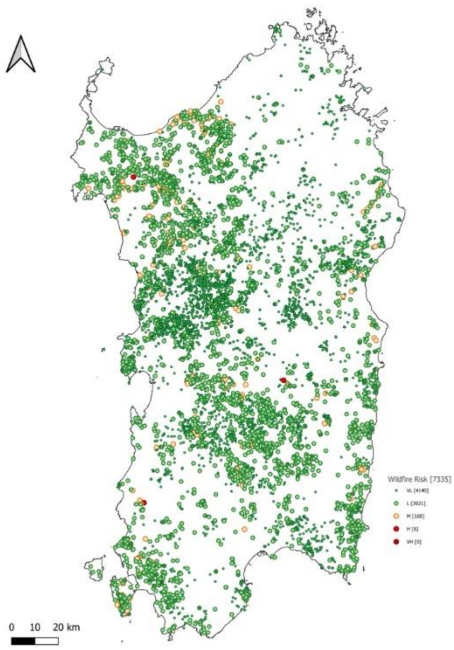

Figure 30. Wildfire risk map.

3.6 Multi-risk at regional scale

The multi-risk analysis for Sardinia was applied to the set of pre-Nuragic and Nuragic monuments. For each monument, the risk values of the four hazards (landslides, floods, earthquakes, wildfires) were combined using two different procedures:

- **National method:** the four risks, previously classified on a five-level scale, were summed. The resulting values, ranging from 0 to 20, were then reclassified into five multi-risk classes with non-uniform intervals (Table 17). This approach reproduces the national framework but applied to a regional extent. Results show that Sardinia tends to present lower multi-risk values compared to other regions, partly due to the generally lower hazard levels (Figure 31).
- **Regional method:** instead of starting from the classified values, the continuous risk values were used. For each monument, the four risks were normalized by the maximum among them, ensuring balanced contribution. The normalized values were summed to obtain a total score between 0 and 4, which was then classified into five evenly spaced classes (Table 18). Results highlight the prevalence of very low and low multi-risk levels, with only six monuments in the high-risk class and none in the very high class (Figure 32). These cases correspond to tall megalithic structures (five circles and one menhir) made of carbonate rocks and located in landslide-prone areas.

Table 17. Multi-risk classification according to the National Method.

0-5	6-8	9-10	11-14	15-20
1	2	3	4	5
VL	L	M	H	VH

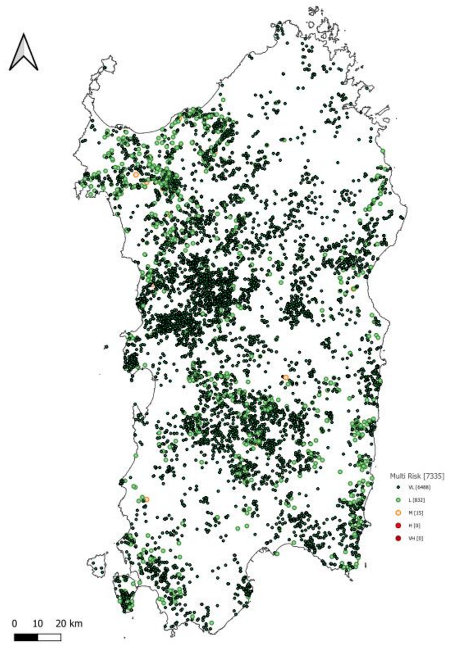

Figure 31. Multi-risk map – National Method.

Table 18. Multi-risk classification according to the Regional Method.

0.0-0.8	0.8-1.6	1.6-2.4	2.4-3.2	3.2-4.0
1	2	3	4	5
VL	L	M	H	VH

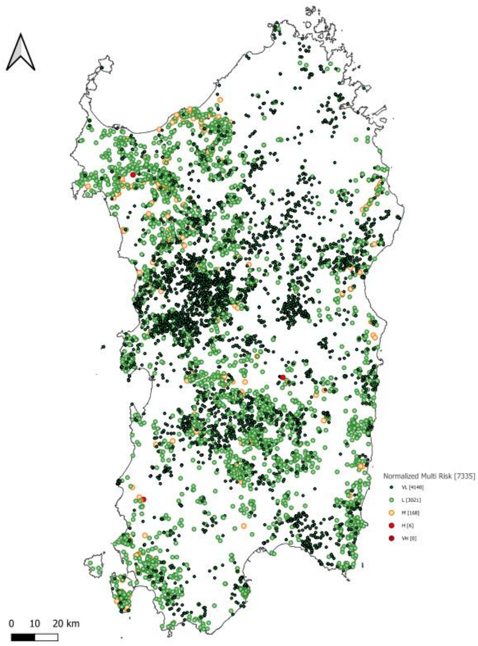

Figure 32. Multi-risk map – Regional Method.

To evaluate the multi-risk values at the municipality level, a spatial analysis was conducted to link each monument with its respective municipality (Figure 33). The multi-risk assessment method for municipalities starts by analyzing individual risks instead of relying on previously calculated multi-risk values for each monument. First, all the monuments are aggregated at the municipal level, and their risk values are summed within each municipality. This total is then divided by the maximum risk value among all municipalities, resulting in four normalized risk values that range from 0 to 1 for each municipality. The multi-risk is calculated by summing these four normalized values, which can result in a range from 0 (if the risk associated with each hazard is zero) to 4 (if all risks are at their maximum of 4). Finally, this continuous value is classified according to a discrete five-level scale, as outlined in Table 19.

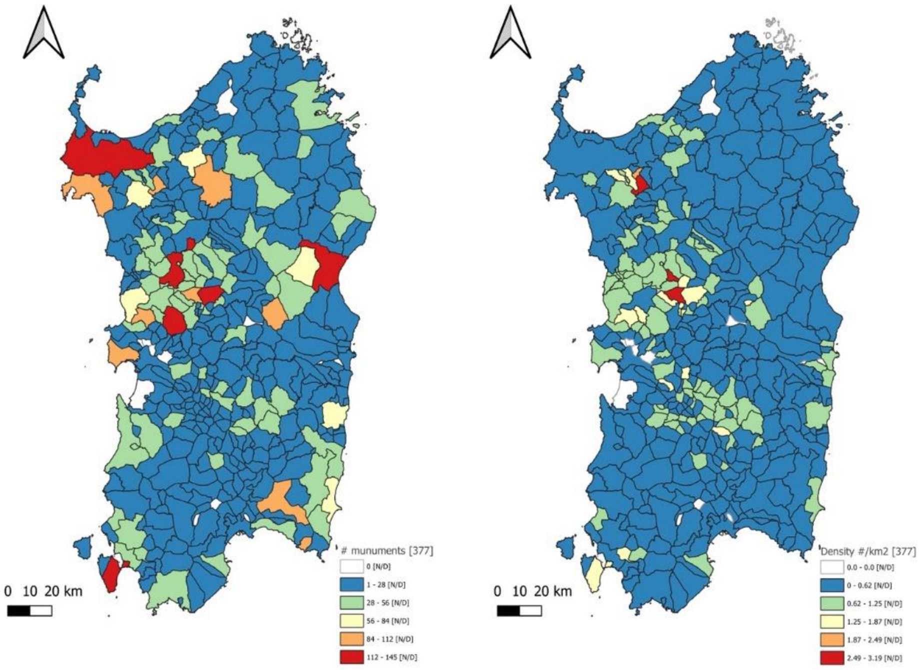

Figure 33. Spatial analysis of the municipalities: number of monuments (left), and density (right).

Table 19. Multi-risk classification of municipalities.

0.0-0.8	0.8-1.6	1.6-2.4	2.4-3.2	3.2-4.0
1	2	3	4	5
VL	L	M	H	VH

Figure 34 displays the multi-risk map at municipality level according to the National Method, along with a pie chart illustrating the percentage of each multi-risk class.

Finanziato dall'Unione europea NextGenerationEU | Ministero dell'Università e della Ricerca | Italiadomani PIANO NAZIONALE DI RIPRESA E RESILIENZA | Return

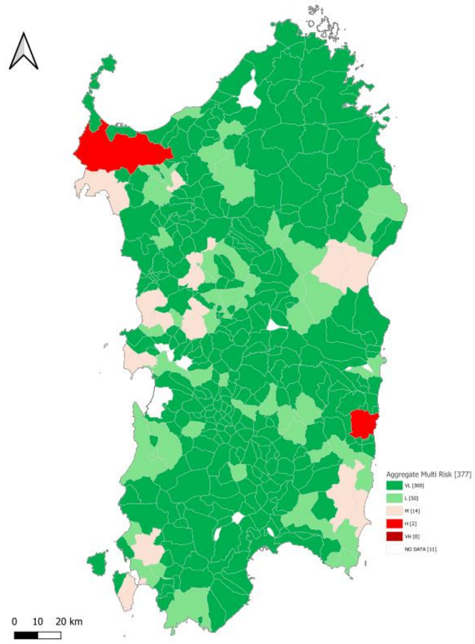

Figure 34. Municipalities multi-risk map.

4 Urban scale

At the urban scale, the methodological framework requires a substantial refinement compared to national applications. The focus shifts from a generalized representation of cultural heritage exposure to the explicit modelling of individual building footprints, which are considered as areal features rather than points. This change in spatial representation allows for a more accurate alignment with hazard layers and enables the use of detailed, site-specific information.

The case study selected for this scale is the historic center of Florence, a UNESCO World Heritage Site since 1982. The choice was motivated by three main factors: (i) the exceptional density and diversity of cultural heritage assets within a limited area, (ii) the availability of harmonized multi-hazard datasets, and (iii) the presence of complementary information on cultural value and visitor flows. These elements make Florence an optimal context to test the adaptability of the methodology to highly complex urban settings.

Compared to the national scale, the urban analysis incorporates higher-resolution hazard models (e.g., hydraulic simulations for floods, local inventories for landslides, building-type classification for seismic vulnerability, and propagation scenarios for wildfires), together with asset-specific attributes such as entrance elevation, structural typology, and visitor statistics. The integration of these datasets into a unified GIS environment provides the basis for a consistent multi-risk assessment at building level, ensuring methodological continuity with the broader-scale approach while enhancing its precision and applicability for local risk management.

4.1 Cultural Heritage Database

The cultural heritage dataset at the urban scale is composed of 41 assets located within the historic center of Florence, all included in the UNESCO World Heritage Site since 1982. The selection of these assets was guided by the availability of consistent and comparable information across the three hazards considered in this study – landslides, flood, earthquake and wildfire – thus ensuring that each building could be assessed under a multi-risk perspective.

The urban-scale dataset adopts an aerial representation. Each building is mapped as a polygon, allowing a more accurate spatial correspondence with hazard layers and enabling the consideration of its geometric extent. This methodological refinement is particularly relevant in dense historical fabrics such as Florence, where building footprints are highly heterogeneous and spatial interactions with hazards may vary significantly even within a single block. Each record corresponds to an individual building and is described by a set of attributes covering its geographical location, architectural typology, and cultural relevance. Specifically, the dataset includes:

- Denomination and typology, distinguishing between religious buildings, museums, towers, and other historical structures.
- Landslide-related fields, including indices from official inventories (PAI and IFFI) and local slope stability assessments, used to identify potential interactions between buildings and slope instabilities.
- Flood-related indicators, namely the expected water depth at the building site under three probabilistic scenarios (return periods of 66, 200, and 500 years), as derived from hydraulic modelling of the Arno River. The database also reports the elevation of the entrance level above the street, a key parameter in flood vulnerability assessment.
- Seismic-related attributes referring to the classification schemes introduced by the national Guidelines for the evaluation and reduction of seismic risk of cultural heritage (MiC).
- Wildfire-related attributes, available for selected exposed sites, where local propagation scenarios were developed to assess potential interactions between vegetation, topography and cultural assets.
- Cultural and socio-economic indicators, including UNESCO Outstanding Universal Value (OUV) designation, estimated annual visitors (from official statistics or regression-based estimations), and inclusion in official cultural itineraries.

Among the 41 selected assets, major landmarks such as the Cathedral of Santa Maria del Fiore, the Campanile di Giotto, the Basilica of Santa Croce and the Uffizi Gallery are included, together with several secondary churches, palaces, and cultural institutions. This heterogeneity reflects both the symbolic and functional variety of the historic center of Florence, while also ensuring the representation of buildings with different structural and social characteristics.

4.2 Hazard

4.2.1 Landslide hazard

At the urban scale, landslide hazard was assessed through the integration of national and regional inventories, combined with local susceptibility zoning. Each cultural heritage asset was considered as a polygonal feature, allowing the direct overlay with hazard maps.

The procedure followed a two-step approach. First, if the footprint of a building intersected an active landslide polygon reported in the national Inventario dei Fenomeni Franosi in Italia (IFFI), the maximum hazard level was assigned (value = 1). This rule reflects the direct evidence of ongoing instability and the consequent high probability of damage to exposed assets.

Second, for all buildings outside IFFI polygons, hazard levels were derived from the Piano di Assetto Idrogeologico (PAI), which provides a classification of landslide-prone areas at municipal scale. PAI classes were converted into normalized hazard scores according to the following weights: P1 = 0.2; P2 = 0.4; P3 = 0.6; P4 = 0.8. This ensured comparability with other hazard indicators and consistency with the multi-hazard framework adopted in the study. The resulting map is shown in Figure 35.

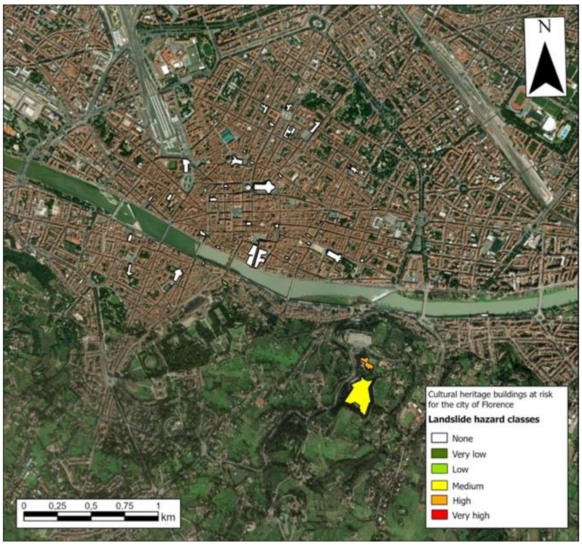

Figure 35. Landslide hazard map at the urban scale.

4.2.2 Flood hazard

The hydraulic model used in this study to simulate flood propagation in the floodplain is HEC-RAS version 5.0.7. A combined 1D/2D modeling approach is employed: the flow within the river channel is calculated using a standard solver for the 1D unsteady flow equations, while the floodplain dynamics are represented using the 2D shallow water equations (SWE). These equations model the movement of water based on depth-averaged 2D velocity and water depth, accounting for gravity and frictional forces. The SWE expresses the conservation of mass and momentum and are solved using the finite-volume method. Flow exchange between the river and floodplain is handled via a system of lateral weirs, with flow over the structures computed using the weir equation. The floodplain is discretized into a grid of cells, each incorporating high-resolution terrain data at 1-meter resolution. Buildings are treated as impermeable blocks. For each cell and cell face, HEC-RAS generates detailed hydraulic property tables (e.g., elevation-volume and elevation-area relationships). Water movement is governed by the local topography and flow resistance, which depends on land use and corresponding Manning's roughness coefficients. Four flood scenarios are modeled, corresponding to exceedance probabilities of 1/30, 1/100, 1/200, and 1/500. For each scenario, the hydrograph with the greatest resulting inundation extent is selected. The output of the hazard model consists of flood depth maps for the study area under the chosen probabilistic scenarios. These values were finally normalized and attributed to the 41 assets in the database, which were reclassified into 5 classes. The result is shown in Figure 36.

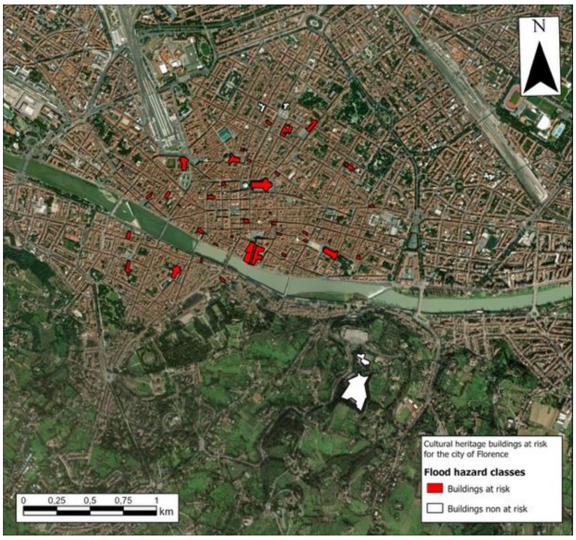

Figure 36. Flood hazard map at the urban scale

4.2.3 Earthquake hazard

At the urban scale, seismic hazard is defined based on the mapping provided by INGV and adopted at the national level. The ag value derived from the grid has been identified according to the urban context of interest. Then, based on soil information from microzonation studies, the coefficient S has been determined in accordance with NTC2018. The S coefficient accounts for both the soil class (Ss) of the area and the topographic conditions (St). At the urban scale, for each CH asset, seismic hazard has been assessed by considering the specific conditions of soil stratification and morphology, moreover the calculation of the value of H was computed together with V. Consequently, the resulting map is shown in paragraph 4.3.3, Figure 41.

4.2.4 Wildfire hazard

At the urban scale, wildfire hazard was assessed through the definition of local propagation scenarios. Unlike floods or earthquakes, fire events are highly dependent on short-term conditions such as vegetation status and meteorological variables, which require site-specific modelling. For this reason, the analysis was restricted to two exposed assets located on the hills south-east of the city center: the Abbey of San Miniato al Monte and the Church of San Salvatore al Monte. These sites were selected due to their cultural importance and their location within a vegetated area potentially exposed to fire ignition and spread, shown in Figure 37.

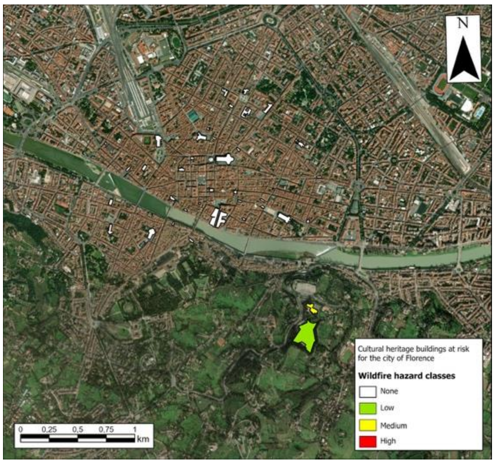

Figure 37. Wildfire hazard map at the urban scale

Wildfire scenarios were generated using the PROPAGATOR cellular automata model (Trucchia et al. 2020). The procedure involved three main steps:

1. Ignition scenario definition, based on expert judgment and the identification of areas with high ignition potential. A worst-case ignition point was selected downslope from the exposed assets and in proximity to the main road network.
2. Static information preparation, including topographic data from the national DEM and vegetation data from the Tuscany Region land cover map (Regione Toscana, 2019). Land cover classes were reclassified into fuel categories following the PROPAGATOR scheme, with particular attention to coniferous vegetation (e.g., the cypress groves surrounding San Miniato), which is highly susceptible to fire spread.
3. Meteorological scenarios, defined from the historical time series of a nearby weather station. Two cases were considered: a "mild" condition (50th percentile of summer values) and an "extreme" condition (90th percentile). Both assumed prevailing north-eastern winds, with wind speeds of 22 km/h and 36 km/h, and fuel moisture levels of 8% and 6%, respectively.

For each configuration, propagation simulations were performed to estimate the probability of fire arrival, arrival time and the potential linear intensity of the flame front. To reduce uncertainty, only areas with a probability of propagation greater than 75% were considered. These outputs provide a spatially explicit characterization of wildfire hazard, which can then be combined with the vulnerability attributes of the exposed buildings to derive risk levels.

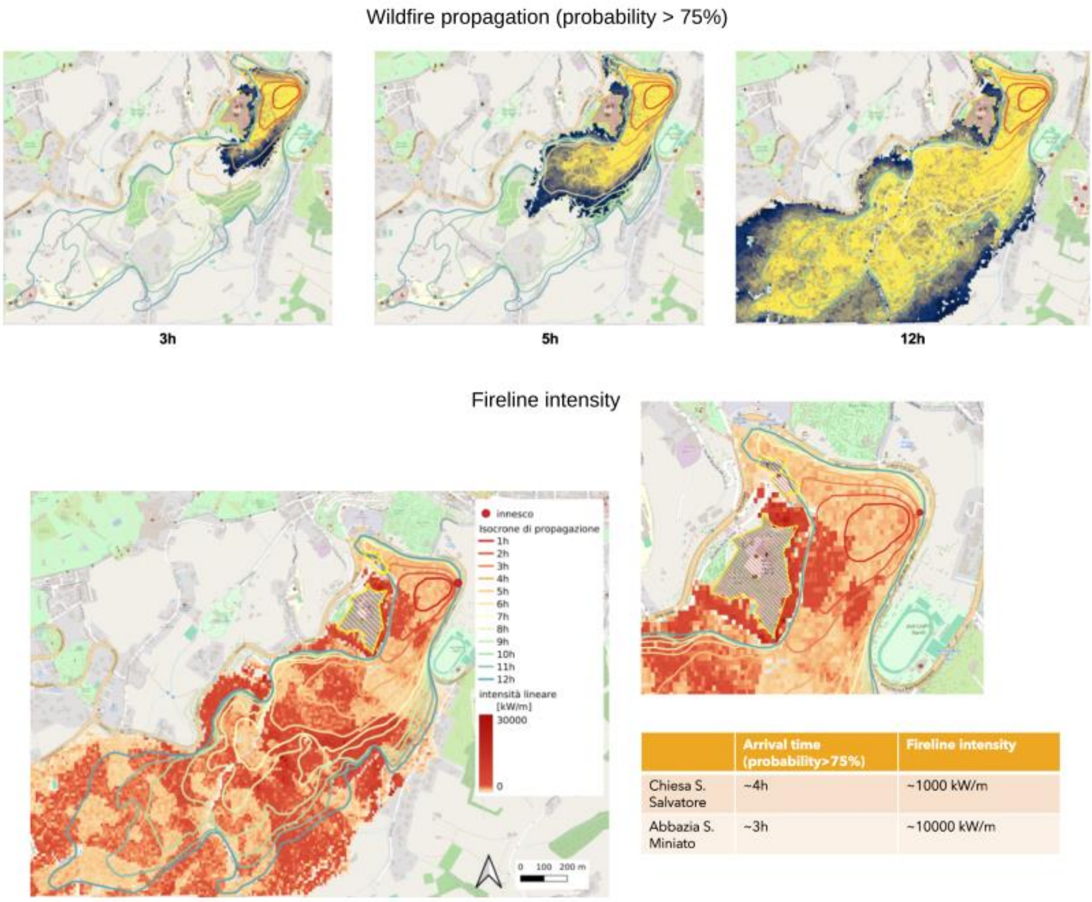

	Arrival time (probability>75%)	Fireline intensity
Chiesa S. Salvatore	~4h	~1000 kW/m
Abbazia S. Miniato	~3h	~10000 kW/m

Figure 38. Wildfire simulation, extreme weather conditions.

4.3 Vulnerability

4.3.1 Landslide vulnerability

The assessment of landslide vulnerability at the urban scale was based on a set of parameters describing the structural and architectural characteristics of cultural heritage assets, complemented by evidence of visible damage where available. The objective was to capture the susceptibility of different building types to ground deformations and slope instabilities, through a weighted classification system.

Four categories of parameters were considered: architectural and urban configuration, foundation typology, masonry typology, and observed damage. Each class within the categories was associated with a relative weight (from 0 to 1) reflecting its contribution to overall vulnerability. Table 20 summarizes the adopted scheme.

This framework allowed the calculation of a landslide vulnerability index for each cultural heritage asset in the Florence case study, shown in

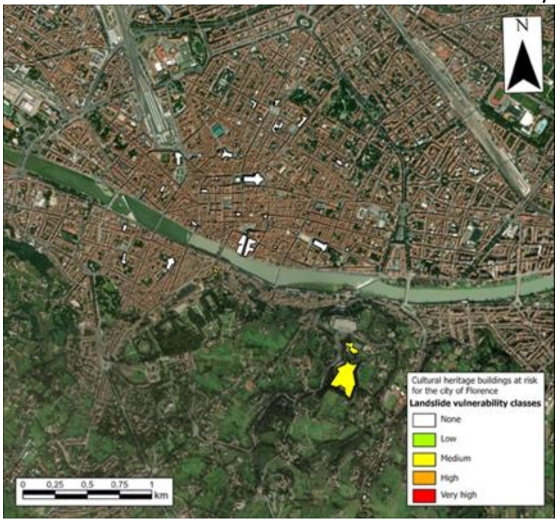

Figure 39. By combining structural attributes (configuration, foundations, masonry) with field evidence of damage, the methodology provides a differentiated representation of how slope instability could impact the urban cultural heritage.

Table 20. Parameters adopted for the assessment of landslide vulnerability of cultural heritage assets at the urban scale.

Category	**Classes**	**Weight**	**Impact on vulnerability**
Architectural and urban configuration	Tower/Bell tower	1.0	Extremely vulnerable to ground displacements due to slender geometry and high aspect ratio
	Isolated building	0.8	Higher sensitivity to differential settlements and tilting due to lack of lateral constraints
	Monumental complex	0.5	Heterogeneous structures with different responses and material discontinuities
	Row (attached) building	0.2	Moderate vulnerability: lateral connections may increase stability but can also lead to cascading damage
Foundation typology	Shallow foundations	1.0	Strongly affected by near-surface soil deformations
	Deep foundations	0.0	Loads transferred to deeper, more stable soil layers
Masonry typology	Rubble or mixed masonry	0.8–1.0	Poor cohesion, irregular texture, highly prone to detachment
	Reinforced concrete/steel frame	0.5	Variable performance, dependent on construction quality and detailing
	Solid brick masonry	0.4	Cohesive but fragile if poorly bonded or lacking ties
	Lightweight timber structure	0.3–0.4	Flexible and adaptable, but sensitive to long-term differential deformation
	Ashlar stone masonry	0.1	Massive but coherent structure, resistant to slow ground movements
	Partial foundation collapse / base shift	1.0	Critical instability leading to potential failure

Observed damage (when available)	Deformation of columns/beams	0.9	Severe impairment of load-bearing members
	Foundation cracks (>1 cm)	0.7	Significant weakening of the base structure
	Floor deformation	0.6	Evidence of settlement or uneven load distribution
	Differential displacement of elements	0.5	Misalignment between walls, beams and slabs
	Structural cracks (>5 mm)	0.4	Moderate indication of stress in load-bearing walls
	Localized settlement	0.3	Limited effects, often not structurally critical

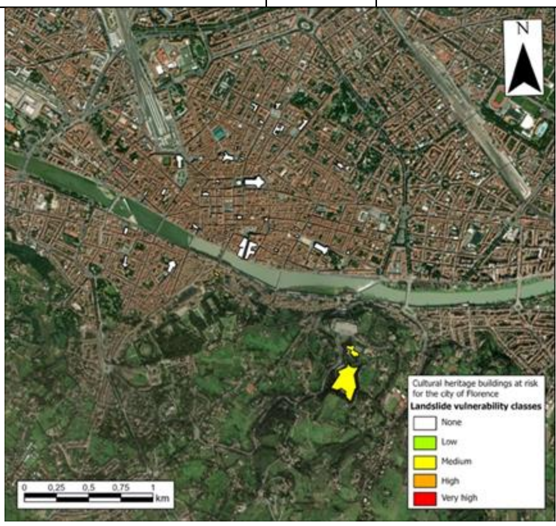

Figure 39. Landslide vulnerability map at the urban scale.

4.3.2 Flood vulnerability

The vulnerability analysis of cultural heritage at the urban scale uses flood depth within buildings as the primary hazard indicator. This is assessed through a statistical analysis of the inundation map within a buffer zone surrounding each building. As a result, specific architectural features—such as the presence of underground floors or elevated entrances above street level—cannot be accounted for at this scale. The scarcity of flood vulnerability functions for cultural heritage is primarily due to the limited availability of empirical data and relevant datasets. The degree of damage is typically assessed based on expert judgement or in a qualitative way, without validation. Consequently, this study adopts the empirical vulnerability model developed by De Lucia et al. (2025), which estimates the degree of tangible loss (LTV)—ranging from slight damage to total destruction—based on the flood depth (MWL) measured outside the building (see Figure 40, left). This model is based on data collected following the 2022 flood event in Italy's Marche region, specifically within the Burano, Cesano, and Misa River catchments. The result of the application of this model to the CH database is shown in Figure 40 (right).

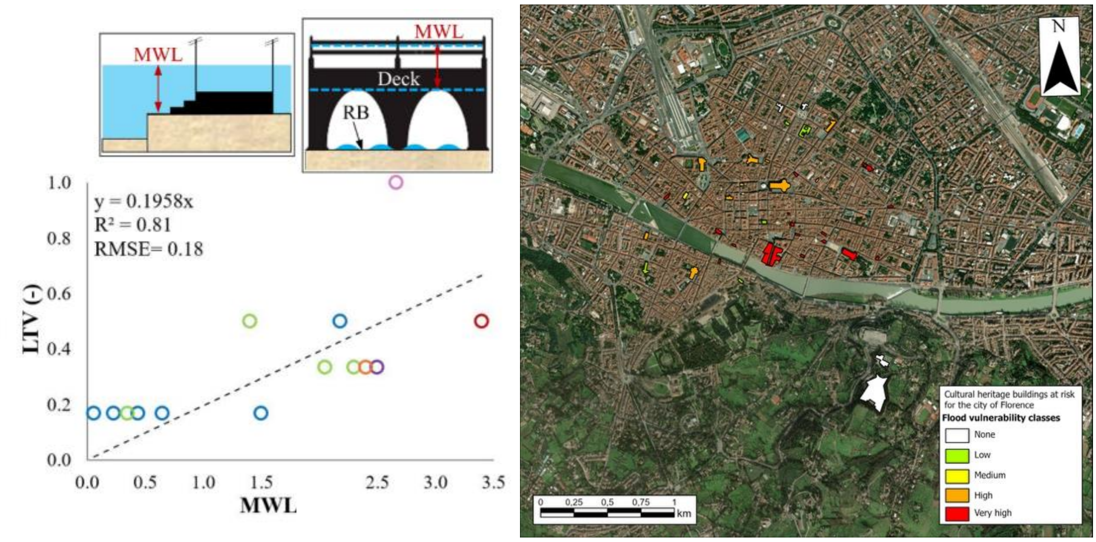

Figure 40. Empirical flood vulnerability function for cultural heritage based of the data collected after the 2022 Marche region flood (left) and flood vulnerability map at the urban scale (right).

4.3.3 Earthquake vulnerability

The "Guidelines for the evaluation and reduction of seismic risk of cultural heritage" have been adopted. They are an operational tool designed to carry out analysis and intervention on cultural heritage buildings exposed to seismic risk.

For the assessment of seismic vulnerability, the Guidelines identify three different levels of increasing completeness: LV1) for seismic safety assessments to be carried out on a territorial scale on all protected cultural heritage assets; LV2) for assessments to be adopted in the presence of local mechanisms on limited portions of the building; LV3) for projects involving interventions that affect the overall structural behavior or when an accurate assessment of the seismic safety of the building is required.

At the urban scale, the analyses have involved palaces and churches throughout the city of Florence. The seismic vulnerability assessment was carried out following the procedure provided for the first level of assessment (LV1). This approach involves simplified procedures that do not require high computational efforts, leading to qualitative and quantitative assessments. Each structural unit is traced back to the four models outlined in the guidelines (churches, palaces, towers, bridges), to which the specific methodologies are applied.

For churches, the assessment was carried out by completing the specific form that collects geometric, structural, conservation, and geotechnical context information. The form requires the analysis of 28 possible local collapse mechanisms, such as macro-element out-of-plane mechanisms, bell tower detachment, etc. For every mechanism, its potential activation and the resulting damage are evaluated. The scores associated with these aspects contribute to the calculation of a vulnerability index, from which the safety index (IS) is derived, ranging from 0 (maximum vulnerability) to 1 (maximum safety).

In the case of palaces, the SIVARS system, developed by MiC, was used. It is based on the compilation of a form that collects geometric, structural, conservation, and geotechnical context information, adapted to the specific typology of these buildings: the presence of elements (such as internal courtyards, loggias, vaults) is considered in the vulnerability assessment. In this case too, a vulnerability index is calculated, which is then transformed into a safety index. The model allows for a rapid and comparable assessment of seismic risk, even for complex and articulated assets such as historic buildings.

The final V parameter was calculated combined with the H value, as previously mentioned. The final result, applied to the CH database is shown in Figure 41.

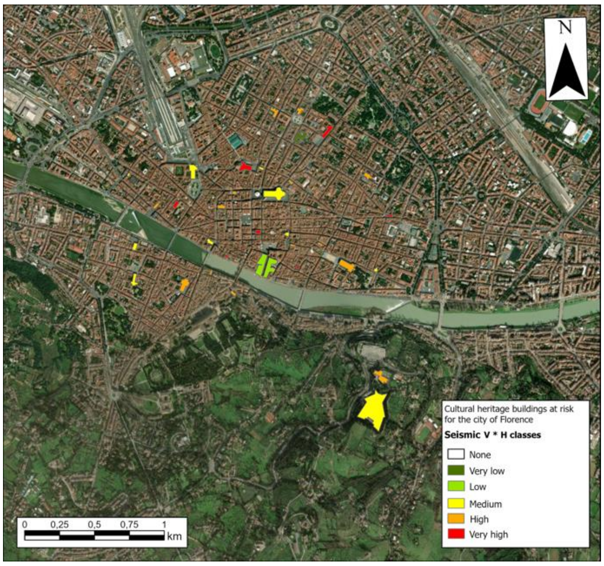

Figure 41 Combined seismic Vulnerability and Hazard map at the urban scale

4.3.4 Wildfire vulnerability

To calculate wildfire vulnerability, we built upon the template used by CAL FIRE (2025) used for building damage assessment under a worst-case scenario, and we adapted it to four fuel type classes:

Grasslands and croplands: 0.1 (nearly negligible expected damage)

Deciduous forests: 0.2 (9% maximum expected damage, low- to medium-intensity surface fires)

Scrublands, shrubs: 0.5 (25% maximum expected damage, minor damage)

Coniferous forests: 1 (potentially crown fires, 50% maximum expected damage, major damage]

These categories are based on the CORINE Land Cover 2018 (Level IV) for the Italian territory (see Table 21 for classification). Some urban-related CORINE classes were included in the "herbaceous vegetation and cultivable land" class for precautionary reasons, also accounting for sparse vegetation. Overlaying the vegetation map with the susceptibility map allows for either exclusion of these areas (if susceptibility is zero) or inclusion (if sparse vegetation results in a non-zero susceptibility); such areas are typically categorized as low-susceptibility fuel classes.

Additionally, agricultural and pastoral landscapes (orchards, rice fields, pastures, etc.) were included in the "herbaceous and cultivable" class. Mixed forests of conifers and broadleaves were classified under "conifers" as a worst-case scenario, since conifers tend to support high-intensity wildfires.

Table 21. Division of CORINE classes on vegetation classes used for fuel mapping.

CORINE class	Description
Grasslands / croplands	
112	Discontinuous urban fabric
121	Industrial, commercial, and public/private service areas
131	Mineral extraction sites
133	Construction sites
132	Dump sites
122	Road and rail networks, engineering works, technical infrastructure
1211	Industrial, artisanal, commercial settlements

123	Port areas
124	Airports
142	Sports and leisure facilities
2111	Non-irrigated arable land – intensive crops
242	Complex cultivation patterns
243	Areas with significant natural spaces within agricultural land
222	Orchards
231	Meadows and alternated pasturelands
241	Temporary crops associated with permanent crops
212	Irrigated arable land
224	Permanent crops
211	Non-irrigated arable land
221	Vineyards
223	Olive groves
213	Rice fields
2112	Extensive crops
321	Natural pastures and grasslands
331	Beaches, dunes, and sand
332	Bare rocks, cliffs, outcrops
3211	Dry calcareous grasslands
3212	Dry siliceous grasslands
333	Areas with sparse vegetation
335	Glaciers and permanent snow
411	Inland marshes
412	Peat bogs
422	Salt pans
421	Saline marshes
522	Estuaries
511	Rivers, canals, waterways
521	Lagoons
Broadleaves	
3111	Holm oak forests
2241	Poplar groves
3112	Deciduous oak forests
3116	Hygrophilous species forests
3117	Exotic broadleaf forests
311	Broadleaf forests
3113	Mesophilous broadleaf forests
3114	Chestnut forests
3115	Beech forests
3131	Mixed forests dominated by broadleaf species

Shrubs	
324	Forest-shrub transition zones
244	Agroforestry areas
323	Sclerophyllous vegetation
334	Burned areas
3241	Shrublands with significant tall shrub and tree presence
3232	Garrigue
322	Maquis
322	Heathlands and shrublands
Conifers	
3123	White and red fir forests
3132	Mixed forests dominated by conifers
312	Conifer forests
3121	Mediterranean pine and cypress forests
3122	Black pine, laricio, Scots pine, Bosnian pine forests
3124	Larch and Swiss pine forests
3125	Exotic conifer forests
313	Mixed conifer and broadleaf forests

Figure 42 shows the distribution of these four vegetation classes across Italy and their respective percentages of burned areas (2007–2023), following the same method used for susceptibility classes. The "herbaceous and cultivable" class is the most represented total area, while shrubs and conifers are the most affected by wildfires.

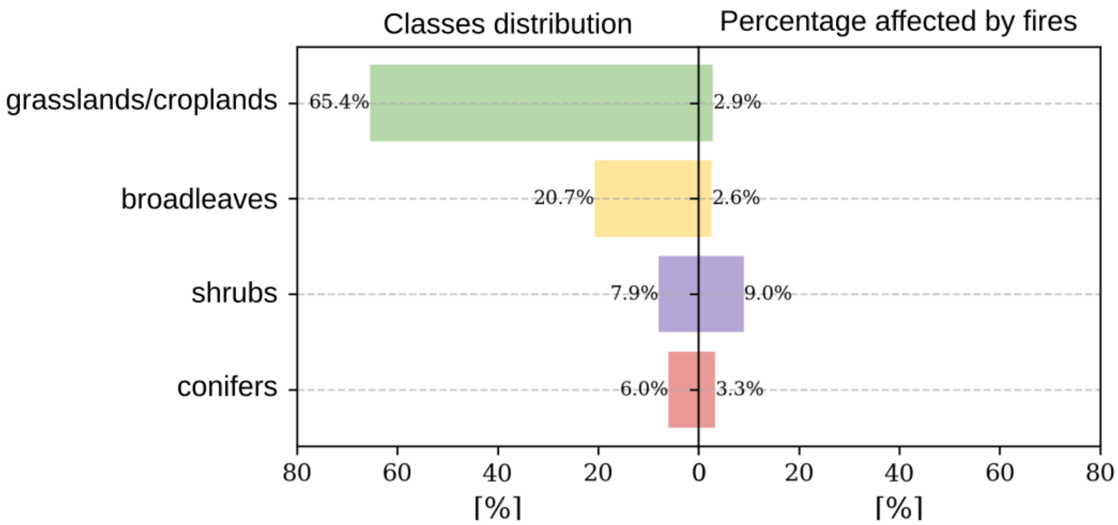

Figure 42. Percentage of coverage of each vegetation class at the national level with respect to the percentage of each class affected by wildfires.

The CH database was subsequently overlaid on the vegetation map, and the vulnerability classes were calculated. The result is shown in Figure 43.

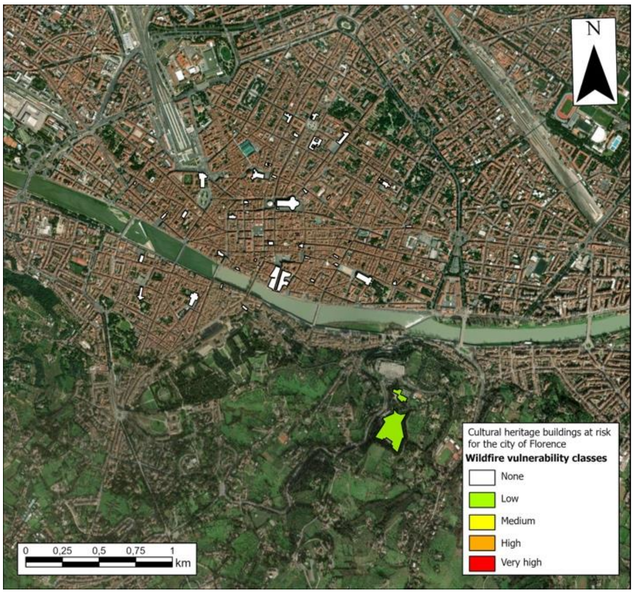

Figure 43. Wildfire vulnerability map at the urban scale

4.4 Exposure

The exposure component of risk was represented through a Cultural Value (CV) Index, designed to quantify the socio-cultural importance of each asset in the historic center of Florence. CV integrates both quantitative and qualitative indicators in order to capture the multiple dimensions of cultural significance that determine the potential impact of hazardous events.

The index is structured around five parameters (Table 22): annual visitors (V), as a proxy for social and economic relevance; average review score (R), reflecting public perception; institutional classification (C), meaning the level of formal designation (international, national, or local); typological relevance (T), which identifies architectural, artistic, or historical value; and inclusion in official itineraries (I), expressing visibility within cultural routes. The five parameters are combined through a weighted linear aggregation, following established methodologies for composite indicator construction. The CV index is calculated as:

$$CV = w_V V + w_R R + w_C C + w_T T + w_I I$$

where the weights are:

$$w_V = w_R = w_C = w_T = w_I = 20\%$$

All variables were normalized on a [0–1] scale and aggregated through a linear model with equal weights, ensuring transparency and comparability.

Missing values for visitor numbers were estimated through a regression model that linked official visitor statistics with Google review counts, in line with recent approaches to exposure modelling in cultural risk frameworks (Arrighi et al., 2022). A subset of 30 cultural buildings was selected for which both of the following were available:

- Total number of Google reviews.
- Verified annual visitor statistics (MIC, 2025b).

A linear model was calibrated to estimate visitor numbers using online reviews as the explanatory variable. The model takes the form:

$$V = \alpha * Total\ reviews + \beta$$

The model achieved a high explanatory power (R^2 = 0.81), ensuring consistent coverage while maintaining methodological robustness. The complete dataset, including the individual parameter values for each of the 41 surveyed buildings together with the final coefficient of variation (CV), is presented in (Table 23).

Parameters C and T are derived from official national heritage registries and institutional cataloguing systems, specifically Vincoli in Rete (MiC, 2025c) and Catalogo Generale dei Beni Culturali (ICCD, 2026), to process administrative and typological data. Parameter C assesses the strategic-governance relevance of the asset by cross-referencing ownership data and protection constraints retrieved from official databases. Within high-profile sites, a value of 1.0 identifies major international attractions that meet specific World Heritage List (OUV) criteria, 0.6 indicates state- or ministry-managed assets, and 0.3 represents the remaining heritage of local or ecclesiastical significance. Parameter T evaluates the density of artistic content and the degree of accessibility, assigning 1.0 to complexes housing absolute masterpieces or museum collections, 0.5 to architectural assets of high quality or those with minor artistic content primarily related to liturgical functions, and 0.1 to purely functional or private buildings lacking accessible collections and closed to the public.

To further explore the structure of cultural values, a multivariate analysis was performed. Principal Component Analysis (PCA) showed that the first three components account for over 90% of total variance, highlighting strong correlations between institutional classification and visitation, as well as between typological relevance and inclusion in itineraries. A subsequent k-means clustering (Figure 44) identified distinct groups of assets, ranging from internationally recognized landmarks with high visitation to marginal buildings with limited accessibility or visibility.

Table 22. CV index components and normalization.

ID	Parameter	Estimation method	Normalization/Scale
V	Annual visitors	Official data (year 2024), or linear regression based on total number of online reviews.	Log-normalization $V = \log(V+1)/\log(V^{max}+1)$
R	Average review score	Average of user ratings (Google Reviews; scale 1–5).	Min-Max scaling
C	Institutional classification	Qualitative categorization based on formal designation.	Fixed values: 1.0 = International relevance (OUV); 0.6 = national/state-level; 0.3 = local/regional significance.
T	Typological relevance	Assessment of architectural, artistic, and historical content.	Fixed values: 1.0/0.5/0.1 depending on cultural features
I	Inclusion in official itineraries	Presence in cultural routes promoted by public institutions (e.g., italia.it)	Binary: 1 = included; 0 = not included

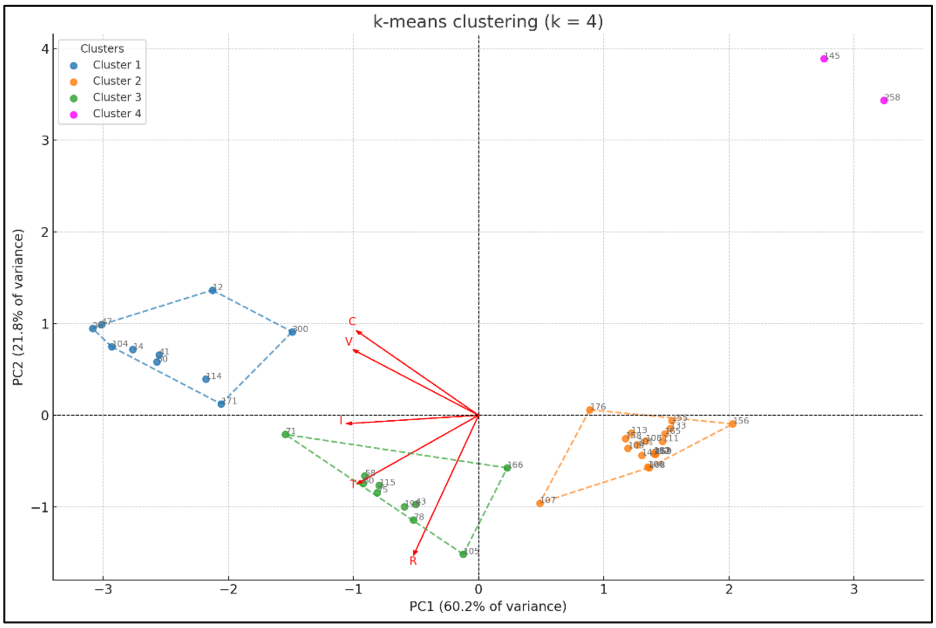

Figure 44. K-means clustering (k = 4) of cultural assets in PCA space. Clusters reflect distinct value profiles based on the five socio-cultural parameters. Red vectors show variable contributions to PC1 and PC2.

Cluster analysis (Figure 44) identified four groups of cultural assets:

1. Cluster 1 (blue): major landmarks with high institutional status, visitor flows and cultural visibility.
2. Cluster 2 (orange): secondary religious sites with limited visibility and lower recognition.
3. Cluster 3 (green): mixed-profile assets with significant content but heterogeneous institutional designation.
4. Cluster 4 (magenta): marginal assets with low accessibility and limited cultural relevance.

The results demonstrate that the CV index is a robust tool for capturing both symbolic and economic aspects of cultural heritage value and thus for defining the exposure parameter in multi-hazard risk assessment.

Table 23. List of the 41 surveyed buildings with the values of each parameter and the corresponding final cultural value (CV).

Name	V	R	C	T	I	CV
Campanile di Giotto	1,0	1,0	1	0,5	1	0,9
Basilica di Santa Croce	0,9	1,0	1	1	1	1,0
Galleria degli Uffizi	1,0	1,0	1	1	1	1,0
Basilica di San Lorenzo	0,9	1,0	1	1	1	1,0
Chiesa S. Maria Maddalena De' Pazzi	0,7	0,9	0,3	1	1	0,7
Galleria dell'Accademia	1,0	1,0	1	1	1	1,0
Chiesa di Santa Maria Novella	0,9	1,0	1	1	1	1,0
Cenacolo di Sant'Apollonia	0,6	1,0	0,6	1	1	0,8

Museo di Orsanmichele	0,8	1,0	0,6	1	1	0,8
Chiesa di Santa Trinita	0,7	1,0	0,3	1	1	0,7
Basilica di San Marco	0,6	1,0	0,3	1	1	0,7
Biblioteca marucelliana	0,6	1,0	0,6	1	1	0,8
Cattedrale di Santa Maria del Fiore	1,0	1,0	1	1	1	1,0
Chiesa di San Salvatore a Ognissanti	0,5	1,0	0,3	1	1	0,7
Chiesa di S. Jacopo Soprarno	0,6	1,0	0,3	0,5	0	0,4
Chiesa di Santa Felicita	0,7	1,0	0,3	1	0	0,5
Chiesa di S. Frediano in Cestello	0,6	0,9	0,3	0,5	0	0,4
Chiesa dei Santi Michele e Gaetano	0,7	1,0	0,3	0,5	0	0,4
Chiesa di San Giuseppe	0,6	0,9	0,3	0,5	0	0,4
Chiesa di Sant'Ambrogio	0,7	0,9	0,3	0,5	0	0,4
Chiesa di Santo Spirito	0,8	1,0	1	1	1	1,0
Chiesa S. Maria del Carmine	0,7	0,9	0,3	1	1	0,7
Chiesa di S. Paolino	0,6	0,9	0,3	0,5	0	0,4
Soprintendenza archivistica per la Toscana (palazzo Neroni)	0,6	0,0	0,6	0,1	0	0,3
Chiesa di San Firenze	0,6	1,0	0,3	0,5	0	0,4
Chiesa S. Margherita in S. Maria De' Ricci	0,6	0,9	0,3	0,5	0	0,4
Compagnia di San Niccolo del Ceppo	0,6	1,0	0,3	0,1	0	0,3
Chiesa di San Simone e Giuda	0,6	1,0	0,3	0,5	0	0,4
Chiesa di Santa Maria Maggiore	0,7	1,0	0,3	0,5	0	0,4
Chiesa di S. Michele Visdomini	0,6	0,9	0,3	0,5	0	0,4
Chiesa dei SS. Apostoli - S. Biagio	0,7	1,0	0,3	0,5	1	0,6
Chiesa di San Remigio	0,6	1,0	0,3	0,5	0	0,4
Chiesa di S. Lucia sul Prato	0,6	1,0	0,3	0,5	0	0,4
Chiesa di Sant'Egidio in S. Maria Nuova	0,6	1,0	0,3	0,5	0	0,4
Basilica della Santissima Annunziata	0,7	1,0	1	1	1	1,0
Chiesa di San Giovannino agli Scolopi	0,6	1,0	0,3	0,5	0	0,4
Biblioteca Palagio di Parte Guelfa	0,6	1,0	0,6	0,5	0	0,5
Chiesa della Badia Fiorentina	0,7	1,0	0,3	1	1	0,7
Palazzo Cocchi	0,6	0,0	0,3	0,1	0	0,1
San Miniato al Monte	0,8	1,0	1	0,5	1	0,9
San Salvatore	0,7	1,0	0,3	0,5	0	0,4

4.5 Risk

Contrarily to the national scale, hazard, vulnerability and exposure calculated for the urban scale were all in the range 0-1. This simplifies the calculation of the risk, since no further normalization is necessary. Therefore, the risk has been calculated as the multiplication of the three parameters (from Figure 45 to Figure 48).

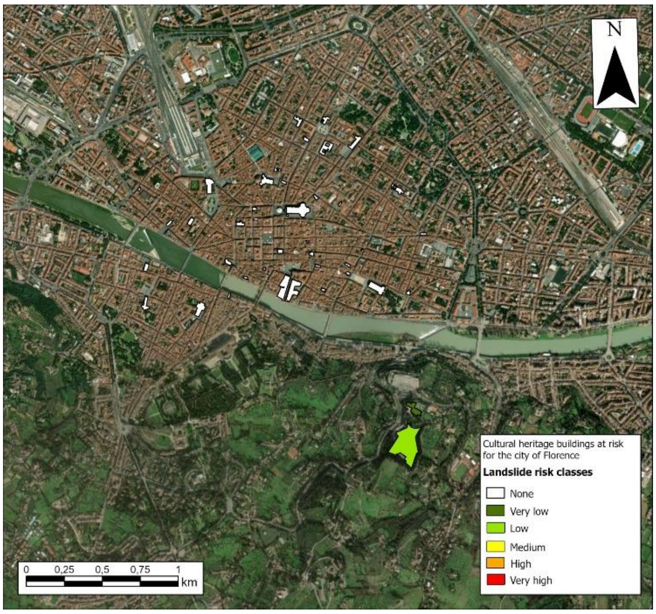

Figure 45. Landslide risk map at the urban scale.

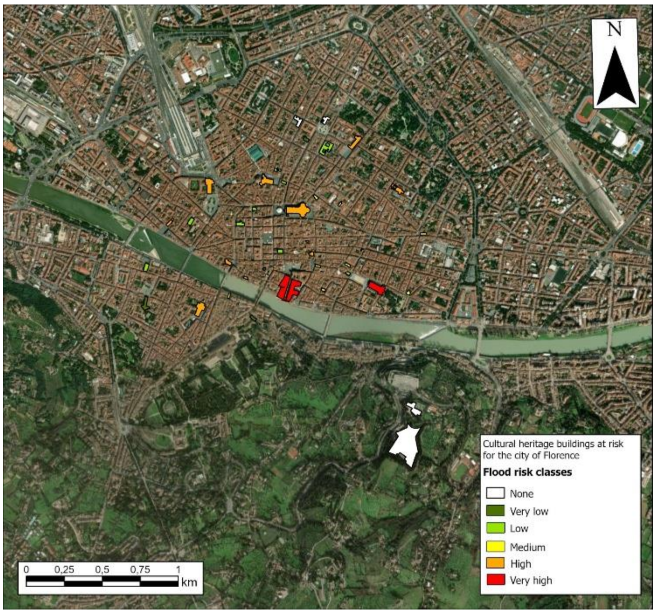

Figure 46. Flood risk map at the urban scale.

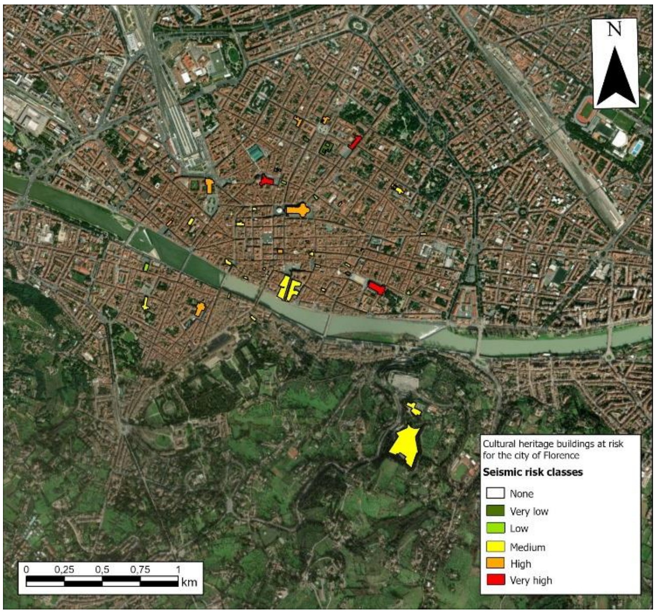

Figure 47. Earthquake risk map at the urban scale.

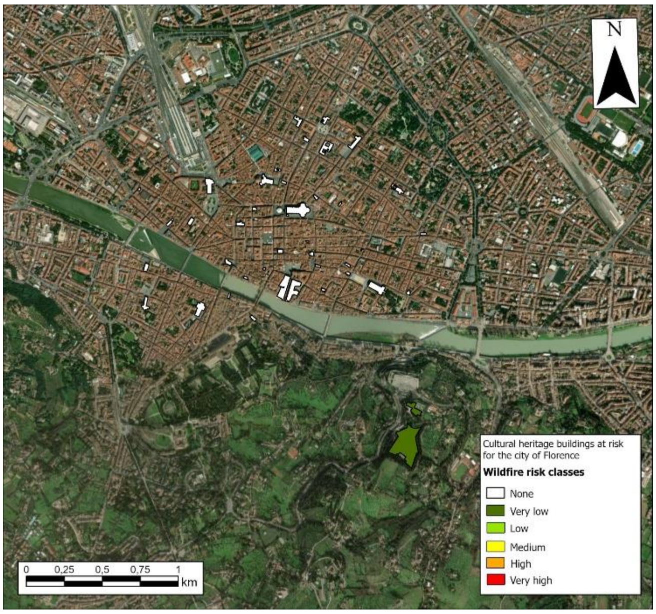

Figure 48. Wildfire risk map at the urban scale.

4.6 Multi-risk at urban scale

The multi-risk has been calculated by summing up the risk values (0-1) for every single type of risk (landslide, flood, earthquake, wildfire). Therefore, the result theoretically ranges from 0 to 4, but since in the Florence PoC the multi-risk values are generally low, the classification has been done using natural breaks to maximize the differences. In fact, differently from the national scale, where the resolution is the single municipality, at the urban scale the resolution is the single cultural heritage asset (in our PoC corresponding to a building); this implies that it is very hard for a building to have an extension wide enough to be affected by all four the types of risk considered. In the

Florence PoC, 39 buildings out of 41 are affected by two types of risk, and only 2 buildings by 3, with flood and landslide risk being almost complementary in spatial terms. Moreover, in the Florence PoC, the single risks are generally low or very low. All of this results in generally low or very low multi-risk values, which required a specific criterion to define the classes.

5 Biosphere reserves

A biosphere reserve (BR) is a protected area of importance for flora, fauna, funga, or features of geological or other special interest, which is reserved and managed for purposes of conservation and to provide special opportunities for study or research. BRs are internationally recognized within the framework of UNESCO's Man and the Biosphere (MaB) Programme. In this context, the human factor plays an increasingly predominant role in relation to ecosystem services. Each BR is intended to fulfill three complementary functions:

- Conservation function: aimed at the preservation of landscapes, habitats, ecosystems, as well as species and genetic diversity.
- Development function: to foster economic and human development, generating not only income but also long-term socio-cultural and environmental sustainability.
- Logistic and support function: to advance the understanding of sustainable development by supporting research, monitoring, and education at the local level, beyond the boundaries of the biosphere reserve, and through the global exchange of best practices.

The three main functions imply that, at the territorial level, Biosphere Reserves are organized into three zones:

- Core Area: a legally designated central area, intended for long-term protection, meeting the conservation objectives of Biosphere Reserves and of sufficient size to fulfil such goals;
- Buffer Zone: an area surrounding or adjacent to the core area, where activities compatible with conservation objectives can take place;
- Transition Area: the outermost area, where sustainable resource management policies are promoted and developed.

For the calculation of multi-hazard risk in BRs, a methodology consistent with the one already applied at the national scale was adopted. The approach is based on the standard risk equation:

$$R = H \times V \times E$$

where H represents hazard, V vulnerability, and E exposure.

BRs represent a peculiar spatial scale that, in spatial terms, are typically between the regional and the urban scales and are not delimited by administrative boundaries. Typically, they are spread over more than one municipality or region, which requires that the input data are homogenized. Since the administrations involved varies for each BR, a standard homogenization procedure, valid for every BR, is difficult to define as it would result in a very complex procedure. An alternative solution is to derive some data from the upper level (national scale).

The PoC chosen for this scale is the Alpi Giulie BR in North-Eastern Italy and every dataset has been resampled as a grid with 100 m x 100 m pixels.

5.1 Hazard

Hazard values were quantified using specific mapping sources for each type of hazard. Due to the reasons explained above, the same databases used for the national scale have been used. Specifically:

- Landslides: based on the Hydrogeological Management Plan (PAI), which classifies areas into four hazard levels (low to very high), assigned numeric values of 0.25, 0.5, 0.75, and 1.
- Floods: based on the Flood Risk Management Plan (PGRA), which distinguishes three levels of increasing hazard, assigned values of 0.2, 0.5, and 1.

- Earthquakes: based on the official INGV (National Institute of Geophysics and Volcanology) map of Peak Ground Acceleration, reclassified into four hazard levels (consistently with the national scale) with corresponding values of 0.25, 0.5, 0.75, and 1.
- Wildfires: based on vegetation fuel types, classified into three hazard levels with values of 0.2, 0.5, and 1, reflecting the energy potential of combustible biomass in case of ignition.

To integrate heterogeneous datasets and enable a comparable spatial analysis, the entire surface of the BR was subdivided into a regular grid (fishnet) of 100 × 100 m cells. Each cell was assigned the corresponding hazard value (H) from the reference layer for the four hazard types through a spatial join procedure in GIS.

5.2 Vulnerability

BRs are defined by a wide set of properties most of which cannot be mapped with precision, either because their exact location is unknown (for example flora or fungi that are not easily mappable at the scale of the single individual) or because they movable (for example wildlife). Moreover, even assuming that the precise spatial distribution of the elements determining the BR designation is known, when considering ecosystems, cascade effects can have severe consequences also when the area interested by that spatial distribution is not directly hit. As an example, an apical predator can suffer damage also if the animals it preys upon are hit.

Therefore, vulnerability differentiated according to the type of hazard and the potential damage each hazard may cause to the BR, as follows:

Earthquakes = 0.1 (although potentially destructive, the predominance of natural ecosystems reduces direct impacts in terms of material damage or casualties)

Landslides and floods = 0.2 (moderate risk, associated with possible soil alteration, suffocation, and material mobilization that may compromise ecosystems)

Wildfires = 1 (as the destruction of vegetation and biotic components represents one of the most severe and immediate threats to the ecological balance of BRs).

5.3 Exposure

Exposure values were derived from the official spatial subdivision of the BR into the three functional zones: Core Zone, Buffer Zone, and Transition Zone. Each zone was assigned an increasing exposure value according to its degree of anthropogenic pressure and ecological sensitivity:

- Core Zone = 1 (highest ecological integrity and protection)
- Buffer Zone = 0.5 (area allowing activities compatible with conservation, such as environmental education, research, and ecotourism; serves as a protective buffer for the Core Zone against external impacts)
- Transition Zone = 0.2 (area with the highest presence of human activities).

5.4 Risk

Since H, V and E range 0-1, also the risk ranges from 0 to 1 (from Figure 49 to Figure 52).

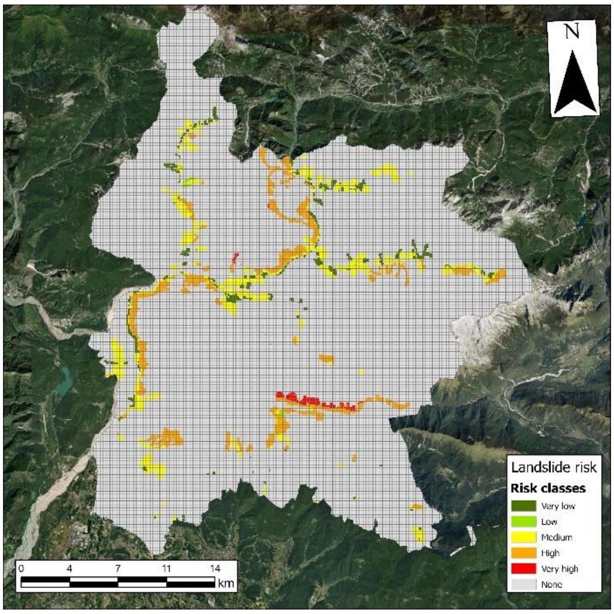

Figure 49. Landslide risk map at the BR scale.

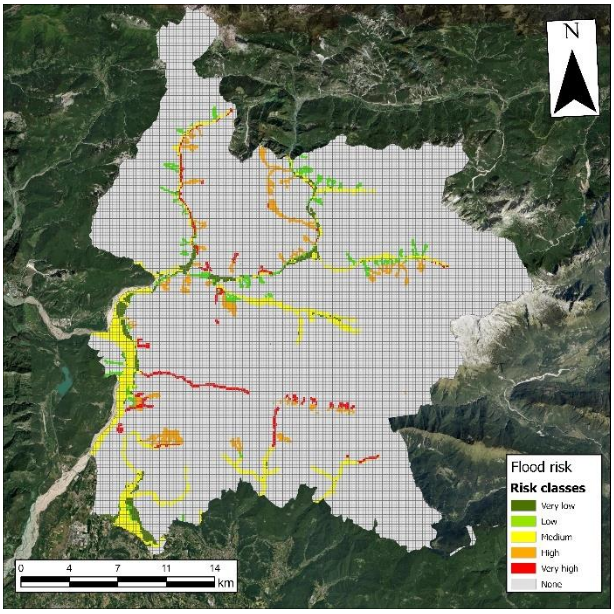

Figure 50. Flood risk map at the BR scale.

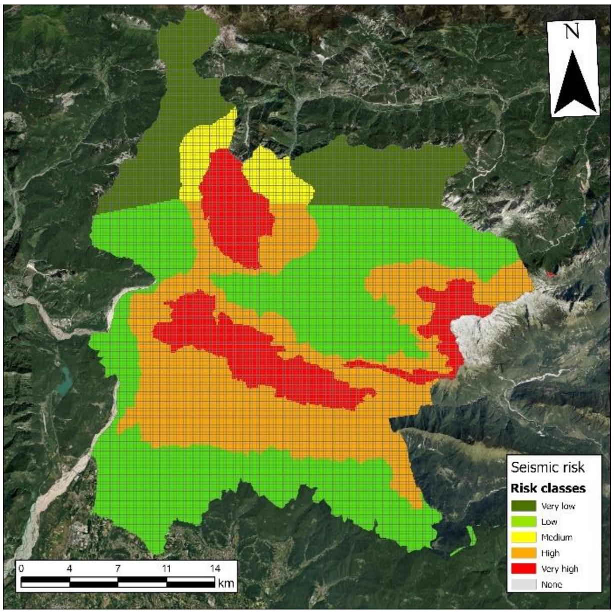

Figure 51. Seismic risk map at the BR scale.

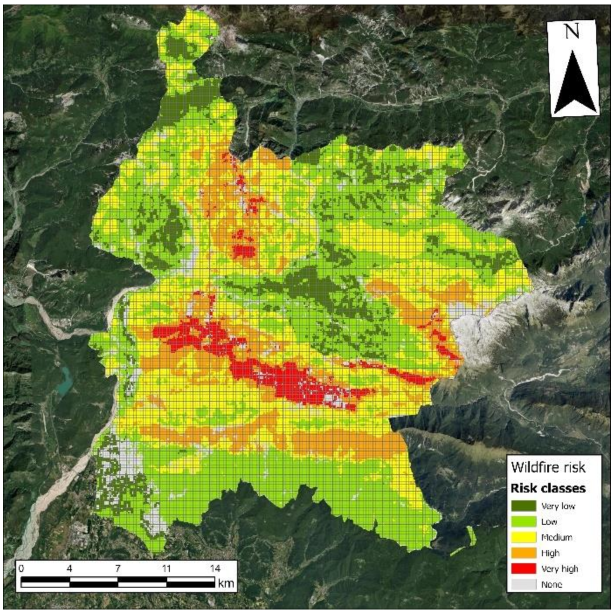

Figure 52. Wildfire risk map at the BR scale.

5.5 Multi-risk

By summing up the risk values for each type of risk, the multi-risk map has been obtained (Figure 53). Wildfire risk is the dominant driver of the multi-risk index, due to its higher vulnerability value. Another key factor is exposure, with the Core Zone showing higher multi-hazard values. Consequently, the exposure, wildfire hazard, and multi-hazard maps present strong spatial similarities.

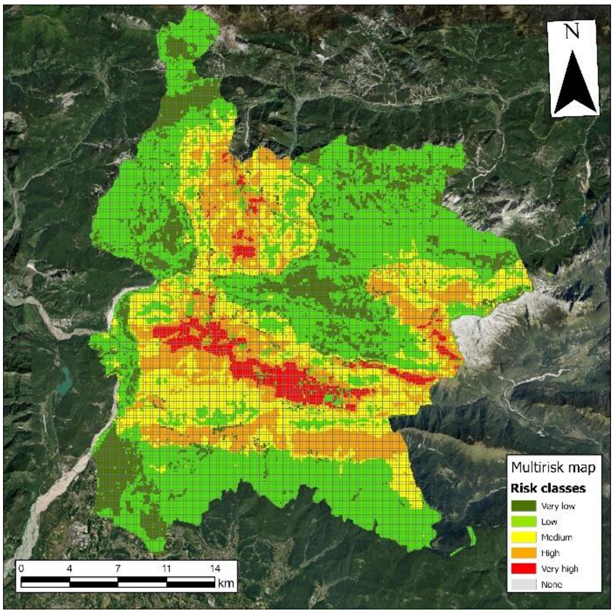

Figure 53. Multi-risk map at the BR scale.

6 References

Anselmi, M., et al. (2020). Microseismic assessment and fault characterization at the Sulcis (South-Western Sardinia) field laboratory. International Journal of Greenhouse Gas Control, 95, 102974. https://doi.org/10.1016/j.ijggc.2019.102974

Arrighi, C., Ballio, F., and Simonelli, T.: A GIS-based flood damage index for CH, Int. J. Disaster Risk Reduct., 90, 103654, https://doi.org/10.1016/j.ijdrr.2023.103654, 2023.

Arrighi, C., Carraresi, A., and Castelli, F.: Resilience of art cities to flood risk: A quantitative model based on depth-idleness correlation, J. Flood Risk Manag., 15, 1–15, https://doi.org/10.1111/jfr3.12794, 2022.

CAL FIRE, 2025. https://gis.data.ca.gov/datasets/1b1c428af1f74a8c912f4b5c9e40d51e/about Last access on July 2025.

Cardil, A., Salis, M., Spano, D., Delogu, G., & Molina Terren, D. (2014). Large wildland fires and extreme temperatures in Sardinia (Italy). iForest - Biogeosciences and Forestry, 7(3), 162–169. https://doi.org/10.3832/ifor1145-007

Copernicus, Global Copernicus Land Cover map, 2025 https://land.copernicus.eu/en/products/global-dynamic-land-cover, Last accessed on July 2025.

De Lucia, C., & Arrighi, C. (2025). Flood vulnerability models for damage assessment of artworks and cultural heritage buildings. *EGUsphere*, 1–32. https://doi.org/10.5194/egusphere-2025-4297

EFFIS (European Forest Fire Information System), 2025, https://effis.jrc.ec.europa.eu/ Last accessed on July 2025.

Figueiredo, R., Romão, X., and Paupério, E.: Flood risk assessment of CH at large spatial scales: Framework and application to mainland Portugal, J. Cult. Herit., https://doi.org/10.1016/j.culher.2019.11.007, 2020.

Garrote, J. and Escudero, C.: A Framework Proposal for Regional-Scale Flood-Risk Assessment of CH Sites and Application to the Castile and Le ó n Region, Water, 12, 329, 2020.

Gorshkov, A., et al. (2021). On the seismic potential of the Corsica-Sardinia block. Rendiconti Lincei. Scienze Fisiche e Naturali, 32, 715–728. https://doi.org/10.1007/s12210-021-00990-z

ICCD (2026). Istituto Centrale per il Catalogo e la Documentazione, Catalogo Generale dei Beni Culturali, Ministero della Cultura. Available at: https://catalogo.beniculturali.it/ Last accessed on February 2026.

INGV, 2025. http://esse1.mi.ingv.it/ Last access on July 2025.

Intrieri, E., Arrighi, C., Bianchini, S., Cardinali, V., Castelli, F., Centauro, I., De Stefano, M., Fiorucci, P., Gatto, A., Marra, A. M., Meschi, G., Segoni, S., Trucchia, A. (2025). Mapping multi-risk for cultural heritage at the national scale (No. EGU25-17319). Copernicus Meetings.

ISIMP (The Inter-Sectoral Impact Model Intercomparison Project) W5E5, 2025 https://www.isimip.org/gettingstarted/input-data-bias-adjustment/details/78/. Last accessed in July 2025.

ISPRA IdroGEO Open Data Available online: https://idrogeo.isprambiente.it/app/page/open-data (accessed on 31 July 2025).

Lagomarsino, S., Podestà, S., & Resemini, S. (2004). Observational and mechanical models for the vulnerability assessment of monumental buildings. Vancouver, B.C., Canada: 13th World Conference on Earthquake Engineering.

Leuenberger M, Parente J, Tonini M, Pereira M G, Kanevski M (2018). Wildfire susceptibility mapping: deterministic vs. stochastic approaches. Environmental Modelling & Software 101, 194-203. https://doi.org/10.1016/j.envsoft.2017.12.019

Meletti, C., Camassi, R., & Castelli, V. (2021). A reappraisal of the seismicity of Sardinia, Italy. Bulletin of the Seismological Society of America, 111(2A), 1148–1158. https://doi.org/10.1785/0120200090

MiC (Ministero della Cultura), 2025a. http://www.cartadelrischio.beniculturali.it Last access on July 2025.

MiC (Ministero della Cultura), 2025b. Visitatori e Introiti di Musei Monumenti e Aree Archeologiche Statali - ANNO 2024. https://statistica.cultura.gov.it/wp-content/uploads/2025/05/MUSEI_TAVOLA7_2024-1.pdf Last access on July 2025.

MiC (Ministero della Cultura), 2025c. Vincoli in Rete. Available at: http://vincoliinrete.beniculturali.it/VincoliInRete/vir/utente/login Last access on February 2026.

Regione autonoma della Sardegna, Piano Stralcio di Bacino per l'Assetto Idrogeologico, *Decreto del Presidente della Regione Sardegna n. 67 del 10/07/2006*

Regione Toscana, Uso e Copertura del Suolo anni 2007-2019, 2019, https://www502.regione.toscana.it/geonetwork/srv/api/records/r_toscan:0d4d6640-9a1c-47a4-9a5d-a85cdb36927c Last accessed in July 2025.

Salis, M., et al. (2015). Analyzing seasonal patterns of wildfire exposure factors in Sardinia, Italy. Environmental Monitoring and Assessment, 187, Article 484. https://doi.org/10.1007/s10661-015-4687-z

Trucchia A, D'Andrea M, Baghino F, Fiorucci P, Ferraris L, Negro D, Gollini A, Severino M (2020). PROPAGATOR: an operational cellular-automata based wildfire simulator. Fire 3, 26. https://doi.org/10.3390/fire3030026

Trucchia A, Meschi G, Fiorucci P, Provenzale A, Tonini M, Pernice U (2023). Wildfire hazard mapping in the eastern Mediterranean landscape. International Journal of Wildland Fire 32, 417-434. https://doi.org/10.1071/WF22138

Yamazaki D, Ikeshima D, Tawatari R, Yamaguchi T, O'Loughlin F, Neal JC, Sampson CC, Kanae S, Bates PD (2017). A high accuracy map of global terrain elevations. Geophysical Research Letters 44, 5844-5853. https://doi.org/10.1002/2017GL072874